[1] **Title:** Carbon cycling in mature and regrowth forests globally: a macroecological synthesis based on the
[2] Global Forest Carbon (ForC) database

[3] **Authors:**

[4] Kristina J. Anderson-Teixeira[1,2]*

[5] Valentine Herrmann[1]

[6] Becky Banbury Morgan[1,3]

[7] Ben Bond-Lamberty[4]

[8] Susan C. Cook-Patton[5]

[9] Abigail E. Ferson[1,6]

[10] Helene C. Muller-Landau[2]

[11] Maria M. H. Wang[1,7]

[12] **Author Affiliations:**

[13] 1. Conservation Ecology Center; Smithsonian Conservation Biology Institute; National Zoological Park,
[14] Front Royal, VA 22630, USA
[15] 2. Center for Tropical Forest Science-Forest Global Earth Observatory; Smithsonian Tropical Research
[16] Institute; Panama, Republic of Panama
[17] 3. School of Geography, University of Leeds, Leeds, UK
[18] 4. Joint Global Change Research Institute, Pacific Northwest National Laboratory, College Park
[19] Maryland 20740, USA
[20] 5. The Nature Conservancy; Arlington VA 22203, USA
[21] 6. College of Natural Resources, University of Idaho; Moscow, Idaho 83843, USA
[22] 7. Grantham Centre for Sustainable Futures and Department of Animal and Plant Sciences, University of
[23] Sheffield, Western Bank, Sheffield, South Yorkshire S10 2TN, UK

[24] *corresponding author: teixeirak@si.edu; +1 540 635 6546

Summary

Background. Forests are major components of the global carbon (C) cycle and thereby strongly influence atmospheric carbon dioxide (CO2) and climate. However, efforts to incorporate forests into climate models and CO_2 accounting frameworks have been constrained by a lack of accessible, global-scale synthesis on how C cycling varies across forest types and stand ages.

Methods/Design. Here, we draw from the Global Forest Carbon Database, ForC, to provide a macroscopic overview of C cycling in the world's forests, giving special attention to stand age-related variation. Specifically, we use 11923 *ForC* records for 34 C cycle vaariables from 865 geographic locations to characterize ensemble C budgets for four broad forest types – tropical broadleaf evergreen, temperate broadleaf, temperate conifer, and taiga. We include estimates for both mature and regrowth (age <100 years) forests, and quantify trends with stand age in regrowth forests for all variables with sufficient data.

Review Results/ Synthesis. The rate of C cycling generally increased from boreal to tropical regions in both mature and regrowth forests, whereas C stocks showed less directional variation. Net ecosystem production of mature forests was indistinguishable across biomes. The majority of flux variables, together with most live biomass pools, increased significantly with stand age when fit with logarithmic functions.

Discussion. As climate change accelerates, understanding and managing the carbon dynamics of forests is critical to forecasting, mitigation, and adaptation. This comprehensive and synthetic global overview of C stocks and fluxes across biomes and stand ages will help to advance these efforts.

Key words: forest ecosystems; carbon cycle; stand age; productivity; respiration; biomass; global

Background

Forest ecosystems are shaping the course of climate change through their influence on atmospheric carbon dioxide (CO_2; Bonan 2008, Friedlingstein *et al* 2019, IPCC 2018). Despite the centrality of forest C cycling in regulating atmospheric CO_2, important uncertainties in climate models (Friedlingstein *et al* 2006, Krause *et al* 2018, Bonan *et al* 2019, Di Vittorio *et al* 2020) and CO_2 accounting frameworks (Pan *et al* 2011) can be traced to lack of understanding on how C cycling varies across forest types and in relation to stand history. This requires accessible, comprehensive, and large-scale databases with global coverage, which runs contrary to the traditional way forest C stocks and fluxes have been measured and published. Large-scale synthesis is critical to benchmarking model performance with global data (Clark et al 2017, Luo et al 2012), quantifying the the role of forests in the global C cycle (*e.g.*, Pan *et al* 2011), and using book-keeping methods to quantify actual or potential exchanges of CO_2 between forests and the atmosphere (Griscom *et al* 2017, Houghton 2020).

Forests in the global C cycle: current and future

A robust understanding of forest impacts on global C cycling is essential. Total annual photosynthesis in forests (gross primary productivity, GPP) is estimated at >69 Gt C yr^{-1} (Badgley *et al* 2019), more than seven times the average annual fossil fuel emissions during 2009-2018 (9.5 ± 0.5 Gt C yr^{-1}; Friedlingstein *et al* 2019). Most of this enormous C uptake is counterbalanced by releases to the atmosphere through ecosystem respiration (R_{eco}) and fire, with forests globally dominant as sources of both soil respiration (Warner *et al* 2019) and fire (van der Werf *et al* 2017). In recent years, total forest C uptake has exceeded releases, such that globally forests have been a C sink. Considering only areas remaining in forest, this C sink has averaged 3.2 ± 0.6 Gt C yr^{-1} for 2009-2018, offsetting 29% of anthropogenic fossil fuel emissions (Friedlingstein *et al* 2019). However, deforestation, estimated at ~1 Gt C yr^{-1} in recent decades (Pan *et al* 2011, Tubiello *et al* 2020), reduces the net forest sink to ~1.1-2.2 Gt C yr^{-1} (Friedlingstein *et al* 2019).

The future of the current forest C sink is dependent both upon forest responses to climate change itself and human land use decisions, which will feedback and strongly influence the course of climate change. Regrowing forests in particular will play an important role (Pugh *et al* 2019), as almost two-thirds of the world's forests were secondary as of 2010 (FAO 2010). As anthropogenic and climate-driven disturbances impact an growing proportion of Earth's forests (Andela *et al* 2017, McDowell *et al* 2020), understanding the carbon dynamics of regrowth forests is increasingly important (Anderson-Teixeira *et al* 2013). Although age trends in aboveground biomass have been relatively well-studied and synthesized globally (Cook-Patton *et al* 2020), a relative dearth of data and synthesis on other C stocks and fluxes in secondary forests points to an under-filled need to characterize age-related trends in forest C cycling. Such understanding is particularly critical for reducing uncertainty regarding the potential for carbon uptake and climate change mitigation by regrowth forests (Krause *et al* 2018, Cook-Patton *et al* 2020). Understanding, modeling, and managing forest-atmosphere CO_2 exchange is thus central to efforts to mitigate climate change (Grassi *et al* 2017, Griscom *et al* 2017, Cavaleri *et al* 2015).

Evolution of forest C cycle research

For more than half a century, researchers have sought to understand how forest carbon cycling varies across stands, including those of different biomes (e.g., Lieth 1973, Luyssaert *et al* 2007) and stand ages (e.g., Odum 1969, Luyssaert *et al* 2008). Over this time, an increasingly refined conceptual understanding of the

elements of ecosystem C cycles has developed, as a growing number of variables have been defined (e.g., Chapin *et al* 2006), along with appropriate measurement methods (e.g., Clark *et al* 2001). New technology has also enabled researchers to directly measure an expanding set of variables, notably including the development of continuous measurements of soil CO_2 efflux (Kuzyakov 2006) and ecosystem-atmosphere CO_2 exchange (Baldocchi *et al* 2001). Measurement techniques have been increasingly standardized; for example, of the biomass allometries that strongly influence estimates of most C cycle variables (e.g., Chojnacky *et al* 2014, Chave *et al* 2014). Further standardization has been made possible through research networks such as ForestGEO (Anderson-Teixeira *et al* 2015, Davies *et al* 2021), NEON (Schimel *et al* 2007), and FLUXNET (Baldocchi *et al* 2001, Novick *et al* 2018). Remote sensing technology has become increasingly useful for global- or regional-scale estimates of a few critical variables (e.g., aboveground biomass, B_{ag}: Saatchi *et al* 2011, Hu *et al* 2016, Spawn *et al* 2020, gross primary productivity, GPP: Li and Xiao 2019), yet measurement and validation of most forest C stocks and fluxes necessarily requires intensive on-the-ground data collection.

Alongside these conceptual and methodological developments, there has been a proliferation of measurements across the world's forests. The result of decades of research on forest C cycling is tens of thousands of records distributed across thousands of scientific articles, varying in data formats, units, measurement methods, *etc.* To address global-scale questions, researchers began synthesizing data into increasingly large databases (e.g., Lieth 1973, Luyssaert *et al* 2007, Bond-Lamberty and Thomson 2010, Anderson-Teixeira *et al* 2016, 2018, Cook-Patton *et al* 2020). The current largest, most comprehensive database on forest C cycling is *ForC* (Anderson-Teixeira *et al* 2016, 2018), which contains published estimates of forest ecosystem C stocks and annual fluxes (>50 variables), with different variables capturing distinct ecosystem pools (e.g., woody, foliage, and root biomass; dead wood) and flux types (e.g, gross and net primary productivity; soil, root, and ecosystem respiration). These data are ground-based measurements, and *ForC* contains associated data required for interpretation (*e.g.*, stand history, measurement methods). Since its most recent publication (Anderson-Teixeira *et al* 2018), *ForC* has grown 129% through the incorporation of two additional large databases that also synthesized published forest C data: the Global Soil Respiration Database (SRDB; Bond-Lamberty and Thomson 2010, Jian *et al* 2020) and the Global Reforestation Opportunity Assessment database (GROA; Cook-Patton *et al* 2020). Following these additions, *ForC* currently contains 39762 records from 10608 plots and 1532 distinct geographic areas representing all forested biogeographic and climate zones, making it ideal for assessing how forest C cycling varies across biomes and with respect to stand age.

Biome differences

Forest C cycling varies enormously across biomes, which cateogrize the world's forests according to major differences in climate, vegetation, *etc.* Since the early 19th century, it has been recognized that climate plays a dominant role in shaping differences among forests on a global scale (Humboldt and Bonpland 1807, Holdridge 1947). Global scale data syntheses have shown that C fluxes including GPP, net primary productivity (NPP), and soil respiration (R_{soil}) decrease with latitude or, correspondingly, increase with mean annual temperature and, to a lesser extent, precipitation (Fig. 1a **REFS**; Lieth 1973, Luyssaert *et al* 2007, Hursh *et al* 2017, Banbury Morgan *et al* n.d.). C stocks of mature forests show less directional variation (Fig. 1a). On average, aboveground biomass (B_{ag}) tends to decrease with latitude, but not as dramatically as fluxes, and with the highest B_{ag} forests in relatively cool, moist temperate regions (Keith *et al* 2009, Smithwick *et al* 2002, Hu *et al* 2016). In contrast, standing and downed dead wood ($DW_{standing}$

4

and DW_{down}, respectively) and the organic layer (OL) tend to accumulate more in colder climates where decomposition is slow relative to NPP (Harmon *et al* 1986, Allen *et al* 2002).

Correlative analyses relating C cycle variables to climate and other environmental variables have recently been taken to a new level through use of machine-learning algorithms that relate ground-based C cycle data to *global data on climate/soils/satellite data*, making it possible to create fine-scale global maps of C cycling [e.g., **REFS**;@warner_spatial_2019; Cook-Patton *et al* (2020)]. *This approach can be particularly effective when paired with satellite data . . . (e.g., aboveground biomass: Saatchi et al 2011, Hu et al 2016, Spawn et al 2020, gross primary productivity, GPP: Li and Xiao 2019,).* Any such analysis is however constrained by the quality and coverage of ground-based estimates of forest C fluxes or stocks. While estimates of some variables (e.g., B_{ag}, GPP, NPP, R_{soil}) are widely available, many remain poorly characterized (e.g., DW; autotrophic respiration, R_{auto}) –even at the coarse resolution of biomes. This is a critical limitation not only for understanding forest C cycling, but also for quantifying climate change mitigation across forest biomes or ecozones [e.g., **REFS**].

Age trends and their variation across biomes

Stand age is another important axis of variation in forest C cycling (Fig. 1b,d). In 1969, E.P. Odum's "The Strategy of Ecosystem Development" laid out predictions as to how forest energy flows and organic matter stocks vary with stand age (Odum 1969). Although the conceptualization of the C cycle in this paper is simplistic by current standards, the paper was foundational in framing the theory around which research on the subject still revolves (Corman *et al* 2019), and the basic framework still holds, albeit with modest modifications (Anderson-Teixeira *et al* 2013). Following stand-clearing disturbance, GPP, NPP, and biomass of leaves ($B_{foliage}$) and fine roots ($B_{root-fine}$) increase rapidly and thereafter remain relatively stable ($B_{foliage}$,$B_{root-fine}$, sometimes GPP) or decline slightly (NPP, sometimes GPP; e.g., *Goulden et al. 2011, ... refs in* Anderson-Teixeira *et al* 2013). The decline in NPP occurs because R_{auto} increases relative to GPP as forests age, corresponding to declining carbon use efficiency with stand age (DeLucia *et al* 2007, Collalti *et al* 2020). Heterotrophic respiration, most of which originates from the soil ($R_{het-soil}$) remains relatively constant with stand age *[Law et al., 2003; Pregitzer & Euskirchen, 2004; Goulden et al., 2011]*, with the result that net ecosystem production ($NEP = GPP - R_{eco}$, where R_{eco} is total ecosystem respiration) is initially negative, increases to a maximum at intermediate ages, and declines thereafter *[Law et al., 2003; Pregitzer & Euskirchen, 2004; Zhou et al., 2006; Baldocchi, 2008; Luyssaert et al., 2008; Amiro et al., 2010; Goulden et al., 2011].* The result is that biomass accumulates rapidly in young forests, followed by a slow decline to near zero in old forests *[Lichstein et al., 2009; Yang et al., 2011; Hember et al., 2012].* While these trends have been subject of fairly recent qualitative review (Anderson-Teixeira *et al* 2013), there is need for a synthetic, quantitative review taking advantage of the greatly expanded data now available.
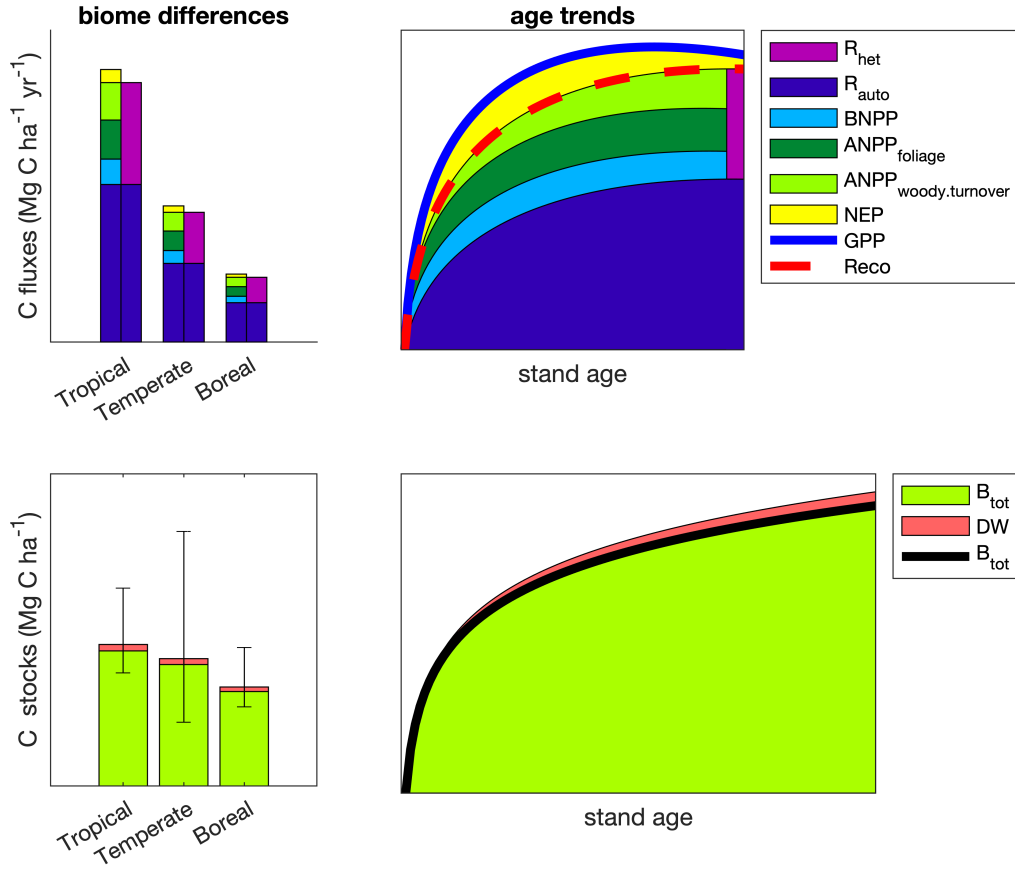
Figure 1 | Schematic diagram summarizing current understanding of biome differences and age trends in forest C cycling. Variables are defined in Table 1. Age trends, which represent idealized dynamics following a disturbance that removes all living and non-living vegetation, are an updated version of the classic figure from Odum (1969), with heavy lines corresponding to those in Odum's figure and NEP corresponding to Odum's 'net production'. Here, NEP conists primarily of woody aboveground net primary production ($ANPP_{woody}$), while $ANPP_{woody.turnover}$ is the sum of woody mortality and branch turnover.

In the past several decades, researchers have started asking how age trends–mostly in B_{ag} or total biomass (B_{tot}) accumulation– vary across biomes. Early research on this theme showed that biomass accumulation rates during secondary succession increase with temperature on a global scale (**REFS**; Anderson *et al* 2006) and *with precipitation in the neotropics* (**REFS**; Poorter *et al* 2016, Chazdon *et al* 2016). Most recently, Cook-Patton *et al* (2020) reinforced these earlier findings with a much larger dataset and crated a high-resolution global map of estimated potential C accumulation rates. However, there has been little synthesis of cross-biome differences in variables other than biomass and its accumulation rate (but see Cook-Patton *et al* (2020) for DW, OL, and soil C accumulation in young stands). Given the important role of secondary forests in the current and future global C cycle, concrete understanding of age trends in C fluxes and stocks and how these vary across biomes is critical to better understanding of the global C cycle. Accurate estimates of C sequestration rates by regrowth forests are also critical for national greenhouse gas accounting under the IPCC framework [**REFS**] and to quantifying the value of regrwoth forests for climate change mitigation (Anderson-Teixeira and DeLucia 2011, Goldstein *et al* 2020).

Here, we conduct a data-based review of carbon cycling from a stand to global level, and by biome and stand

age, using the largest global compilation of forest carbon data, which is available in our open source Global Carbon Forest database (*ForC*; Fig. 2). Our goal is to provide a comprehensive synthesis on broad trends in forest C cycling that can serve as a foundation for improved understanding of global forest C cycling and highlight where key sources of uncertainty still reside.
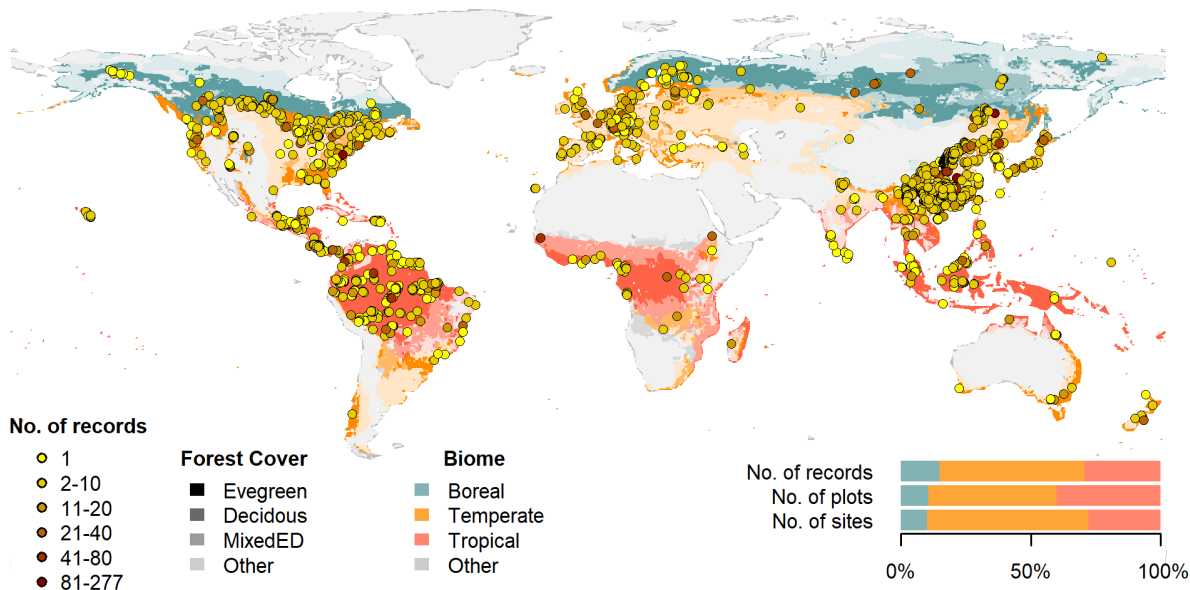

Figure 2 | Map of sites included in this analysis. Symbols are colored according to the number of records at each site. Underlying map shows coverage of evergreen, deciduous, and mixed forests (shading differences; data from Jung et al. 2006) and biomes (color differences). Distribution of sites, plots, and records among biomes is shown in the inset.

Methods/ Design

This review synthesizes data from the *ForC* database (Fig. 2; https://github.com/forc-db/ForC; Anderson-Teixeira *et al* 2016, 2018). *ForC* amalgamates numerous intermediary data sets (*e.g.*, Luyssaert *et al* 2007, Bond-Lamberty and Thomson 2010, Cook-Patton *et al* 2020) and original studies. Original publications were referenced to check values and obtain information not contained in intermediary data sets, although this process has not been completed for all records. The database was developed with goals of understanding how C cycling in forests varies across broad geographic scales and as a function of stand age. As such, there has been a focus on incorporating data from regrowth forests (*e.g.*, Anderson *et al* 2006, Martin *et al* 2013, **???**) and obtaining stand age data when possible (83% of records in v.2.0; Anderson-Teixeira *et al* 2018). Particular attention was given to developing the database for tropical forests (Anderson-Teixeira *et al* 2016), which represented roughly one-third of records in *ForC* v2.0 (Anderson-Teixeira *et al* 2018). Since publication of ForC v2.0, we imported three large additional databases into *ForC* via a combination of R scripts and manual edits. First, we imported (via R script) the Global Database of Soil Respiration Database (*SRDB* v4, 9488 records; Bond-Lamberty and Thomson 2010), and corrections and improvements to *SRDB* arising from this process were incorporated in *SRDB* v5 (Jian *et al* 2020). Second, we imported (via R script) the Global Reforestation Opportunity Assessment database

(*GROA* v1.0, 10116 records; Cook-Patton *et al* 2020, Anderson-Teixeira *et al* 2020), which itself had drawn on an earlier version of *ForC*. Because all records in *GROA* were checked against original publications, these records were given priority over duplicates in *ForC*. Third, we manually incorporated records of annual NEP, GPP, and R_{eco} from the FLUXNET2015 dataset (Pastorello *et al* 2020), treating these records as authoritative when they duplicated earlier records (Appendix S1). We have also added data from individual publications, with a particular focus on productivity (e.g., Taylor *et al* 2017), dead wood, and ForestGEO sites (e.g., Lutz *et al* 2018, Johnson *et al* 2018). A record of data sets added to *ForC* over the course of its development is available at https://github.com/forc-db/ForC/blob/master/database_management_records/ForC_data_additions_log.csv. The database version used for this analysis has been tagged as a new release on Github (v3.0) and assigned a DOI through Zenodo (DOI: TBD).

All measurements originally expressed in units of dry organic matter (OM) were converted to units of C using the IPCC default of $C = 0.47 * OM$ (IPCC 2018). Duplicate or otherwise conflicting records were purged as described in Appendix S1, resulting in a total of 22265 records (56% size of total database). Records were filtered to remove plots that had undergone significant anthropogenic management or major disturbance since the most recent stand initiation event. Specifically, we removed plots with any record of managements manipulating CO_2, temperature, hydrology, nutrients, or biota, as well as any plots whose site or plot name contained the terms "plantation", "planted", "managed", "irrigated", or "fertilized" (13.9% of duplicate-purged records). We also removed stands that had undergone any notable anthropogenic thinning or partial harvest (5.6% of duplicate-purged records). We retained sites that were grazed or had undergone low severity natural disturbances (<10% mortality) including droughts, major storms, fires, and floods. We removed all plots for which no stand history information had been retrieved (5.7%). In total, this resulted in 17349 records (43.6% of the records in the database) being eligible for inclusion in the analysis.

We selected 23 annual flux and 11 C stock variables for inclusion in the analysis (Table 1). These different flux and stock variables represent different pools (e.g., aboveground biomass, root biomass, dead wood) and levels of combination (e.g., total net primary productivity, NPP, versus the individual elements of NPP such as foliage, roots, and branches). Note that two flux variables, aboveground heterotropic respiration (R_{het-ag}) and total respiration (R_{het}), were included for conceptual completeness but had no records in *ForC* (Table 1). Records for our focal variables represented 90.3% of the total records eligible for inclusion. For this analysis, we combined some of ForC's specific variables into more broadly defined variables. Specifically, net ecosystem exchange (measured by eddy-covariance; Baldocchi *et al* 2001) and biometric estimates of NEP were combined into the single variable NEP (Table 1). Furthermore, for NPP, aboveground NPP ($ANPP$), and the litterfall component of $ANPP$ ($ANPP_{litterfall}$), *ForC* variables specifying inclusion of different components were combined (*e.g.*, measurements including or excluding fruit and flower production and herbivory). Throughout ForC, for all measurements drawing from tree census data (*e.g.*, biomass, productivity), trees were censused down to a minimum diameter breast height (DBH) threshold of 10 cm or less. All records were measured directly or derived from field measurements.

We grouped forests into four broad biome types based on climate zones and dominant vegetation type (tropical broadleaf, temperate broadleaf, temperate needleleaf, and boreal needleleaf) and two age classifications (young and mature). Climate zones (Fig. 2) were defined based on site geographic coordinates according to Köppen-Geiger zones (Rubel and Kottek 2010). We defined the tropical biome as including all equatorial (A) zones, temperate biomes as including all warm temperate (C) zones and warmer snow

Table 1. Carbon cycle variables included in this analysis, their sample sizes, and summary of biome differences and age trends.

Variable	Description	records	plots	geographic areas	biome differences*	age trend†
Annual fluxes						
NEP	net ecosystem production or net ecosystem exchange (+ indicates C sink)	329	146	88	n.s.	+; xB
GPP	gross primary production ($NPP + R_{auto}$ or $R_{eco} + NEP$)	303	115	84	TrB > TeB ≥ TeN ≥ BoN	+; xB
NPP	net primary production ($ANPP + BNPP$)	214	112	74	TrB > TeB ≥ TeN > BoN	n.s.
$ANPP$	aboveground NPP	343	236	131	TrB > TeB ≥ TeN > BoN	+; xB
$ANPP_{woody}$	woody production ($ANPP_{stem} + ANPP_{branch}$)	64	53	37	n.s.	+
$ANPP_{stem}$	woody stem production	217	190	117	TrB > TeN ≥ TeB ≥ BoN	n.s.
$ANPP_{branch}$	branch turnover	69	59	42	TrB > TeB ≥ TeN	n.s.
$ANPP_{foliage}$	foliage production, typically estimated as annual leaf litterfall	162	132	88	TrB > TeB ≥ TeN > BoN	+
$ANPP_{litterfall}$	litterfall, including leaves, reproductive structures, twigs, and sometimes branches	82	70	55	n.s.	+
$ANPP_{repro}$	production of reproductive structures (flowers, fruits, seeds)	51	44	34	n.t.	n.t.
$ANPP_{folivory}$	foliar biomass consumed by folivores	20	12	11	n.t.	n.t.
M_{woody}	woody mortality–i.e., B_{ag} of trees that die	18	18	18	n.t.	n.t.
$BNPP$	belowground NPP ($BNPP_{coarse} + BNPP_{fine}$)	148	116	79	TrB > TeN ≥ TeB ≥ BoN	+
$BNPP_{coarse}$	coarse root production	77	56	36	TeN ≥ TrB	n.s.
$BNPP_{fine}$	fine root production	123	99	66	n.s.	+
R_{eco}	ecosystem respiration ($R_{auto} + R_{het}$)	213	98	70	TrB > TeB ≥ TeN	+
R_{auto}	autotrophic respiration ($R_{auto-ag} + R_{root}$)	24	23	15	n.t.	n.t.
$R_{auto-ag}$	aboveground autotrophic respiration (i.e., leaves and stems)	2	2	1	n.t.	n.t.
R_{root}	root respiration	181	139	95	TrB ≥ TeB	+
R_{soil}	soil respiration ($R_{het-soil} + R_{root}$)	627	411	229	TrB > TeB > TeN ≥ BoN	n.s.
$R_{het-soil}$	soil heterotrophic respiration	197	156	100	TrB > TeB ≥ TeN	n.s.
R_{het-ag}	aboveground heterotrophic respiration	0	0	0	-	-
R_{het}	heterotrophic respiration ($R_{het-ag} + R_{het-soil}$)	0	0	0	-	-
Stocks						
B_{tot}	total live biomass ($B_{ag} + B_{root}$)	188	157	87	TrB ≥ TeB > BoN	+; xB
B_{ag}	aboveground live biomass ($B_{ag-wood} + B_{foliage}$)	4466	4072	621	TrB ≥ TeN ≥ TeB > BoN	+; xB
$B_{ag-wood}$	woody component of aboveground biomass	115	102	64	TeN > TrB ≥ BoN	+; xB
$B_{foliage}$	foliage biomass	134	115	72	TeN > TrB ≥ BoN ≥ TeB	+; xB
B_{root}	total root biomass ($B_{root-coarse} + B_{root-fine}$)	2329	2298	360	n.s.	+; xB
$B_{root-coarse}$	coarse root biomass	134	120	73	TeN > TeB ≥ BoN	+; xB
$B_{root-fine}$	fine root biomass	226	180	109	n.s.	+; xB
DW_{tot}	deadwood ($DW_{standing} + DW_{down}$)	79	73	42	n.t.	+; xB
$DW_{standing}$	standing dead wood	36	35	22	n.t.	n.t.
DW_{down}	fallen dead wood, including coarse and sometimes fine woody debris	278	265	37	n.t.	+; xB
OL	organic layer / litter/ forest floor	474	413	115	n.s.	+; xB

* TrB: Tropical, TeB: Temperate Broadleaf, TeN: Temperate Needleleaf, BoN: Boreal, n.s.: no significant differences, n.t.: not tested
† + or -: significant positive or negative trend, xB: significant age x biome interaction, n.s.: no significant age trend, n.t.: not tested

234 climates (Dsa, Dsb, Dwa, Dwb, Dfa, and Dfb), and the boreal biome as including the colder snow climates
235 (Dsc, Dsd, Dwc, Dwd, Dfc, and Dfd). Any forests in dry (B) and polar (E) Köppen-Geiger zones were

excluded from the analysis. We defined leaf type (broadleaf / needleleaf) based on descriptions in original publications (prioritized) or values extracted from a global map based on satellite observations (SYNMAP; Jung *et al* 2006). For young tropical forests imported from *GROA* but not yet classified by leaf type, we assumed that all were broadleaf, consistent with the rarity of naturally regenerating needleleaf forests in the tropics. We also classified forests as "young" (< 100 years) or "mature" (≥ 100 years or classified as "mature", "old growth", "intact", or "undisturbed" in original publication). Assigning stands to these groupings required the exclusion of records for which *ForC* lacked geographic coordinates (0.4% of sites in full database) or records of stand age (5.7% of records in full database). We also excluded records of stand age = 0 year (0.8% of records in full database). In total, our analysis retained 76.1 of the focal variable records for forests of known age. Numbers of records by biome and age class are given in Table S1.

Data were summarized to produce schematics of C cycling across the eight biome by age group combinations identified above. To obtain the values reported in the C cycle schematics, we first averaged any repeated measurements within a plot. Values were then averaged across geographically distinct areas, defined as plots clustered within 25 km of one another (*sensu* Anderson-Teixeira *et al* 2018), weighting by area sampled if available for all records. This step was taken to avoid pseudo-replication.

We tested whether the C budgets described above "closed"–*i.e.*, whether they were internally consistent. Specifically, we first defined relationships among variables: for example, $NEP = GPP - R_{eco}$, $BNPP = BNPP_{coarse} + BNPP_{fine}$, $DW_{tot} = DW_{standing} + DW_{down}$). Henceforth, we refer to the variables on the left side of the equation as "aggregate" fluxes or stocks, and those that are summed as "component" fluxes or stocks, noting that the same variable can take both aggregate and component positions in different relationships. We considered the C budget for a given relationship "closed" when component variables summed to within one standard deviation of the aggregate variable.

To test for differences across mature forest biomes, we also examined how stand age impacted fluxes and stocks, employing a mixed effects model ("lmer" function in "lme4" R package; Bates *et al* 2015) with biome as fixed effect and plot nested within geographic.area as random effects on the intercept. When Biome had a significant effect, we looked at a Tukey's pairwise comparison to see which biomes were significantly different from one another. This analysis was run for variables with records for at least seven distinct geographic areas in more than one biome, excluding any biomes that failed this criteria (Table 1).

To test for age trends in young (<100yrs) forests, we employed a mixed effects model with biome and log10[stand.age] as fixed effects and plot nested within geographic.area as a random effect on the intercept. This analysis was run for variables with records for at least three distinct geographic areas in more than one biome, excluding any biomes that failed this criteria (Table 1). When the effect of stand age was significant at $p \leq 0.05$ and when each biome had records for stands of at least 10 different ages, a biome $\times$ stand.age interaction was included in the model.

To facilitate the accessibility of our results and data, and to allow for rapid updates as additional data become available, we have automated all database manipulation, analyses, and figure production in R (Team 2020).

Review Results/ Synthesis

Data Coverage

Of the 39762 records in *ForC* v3.0, 11923 met our strict criteria for inclusion in this study (Fig. 2). These records were distributed across 5062 plots in 865 distinct geographic areas. Of the 23 flux and 11 stock variables mapped in these diagrams, *ForC* contained sufficient mature forest data for inclusion in our statistical analyses (*i.e.*, records from ≥ 7 distinct geographic areas) for 20 fluxes and 9 stocks in tropical broadleaf forests, 15 fluxes and 8 stocks in temperate broadleaf forests, 14 fluxes and 7 stocks in temperate conifer forests, and 8 fluxes and 7 stocks in boreal forests. For regrowth forests ($<$100 yrs), *ForC* contained sufficient data for inclusion in our statistical analyses (*i.e.*, records from ≥ 3 distinct geographic areas) for 11 fluxes and 10 stocks in tropical broadleaf forests, 16 fluxes and 10 stocks in temperate broadleaf forests, 16 fluxes and 10 stocks in temperate conifer forests, and 14 fluxes and 9 stocks in boreal forests.

C cycling in mature forests

Average C cycles for mature tropical broadleaf, temperate broadleaf, temperate conifer, and boreal forests $\geq$ 100 years old and with no known major natural or anthropogenic disturbance are presented in Figures 2-5 (and available in tabular format in the *ForC* release accompanying this publication: `ForC/numbers_and_facts/ForC_variable_averages_per_Biome.csv`).

For variables with records from ≥ 7 distinct geographic areas, these ensemble C budgets were generally consistent. That is, component variables summed to within one standard deviation of their respective aggregate variables in all but one instance. In the temperate conifer biome, the average composite measure of root biomass (B_{root}) was less than the combined average value of coarse and fine root biomass ($B_{root-coarse}$ and $B_{root-fine}$, respectively). This lack of closure was driven by very high estimates of $B_{root-coarse}$ from high-biomass forests of the US Pacific Northwest.
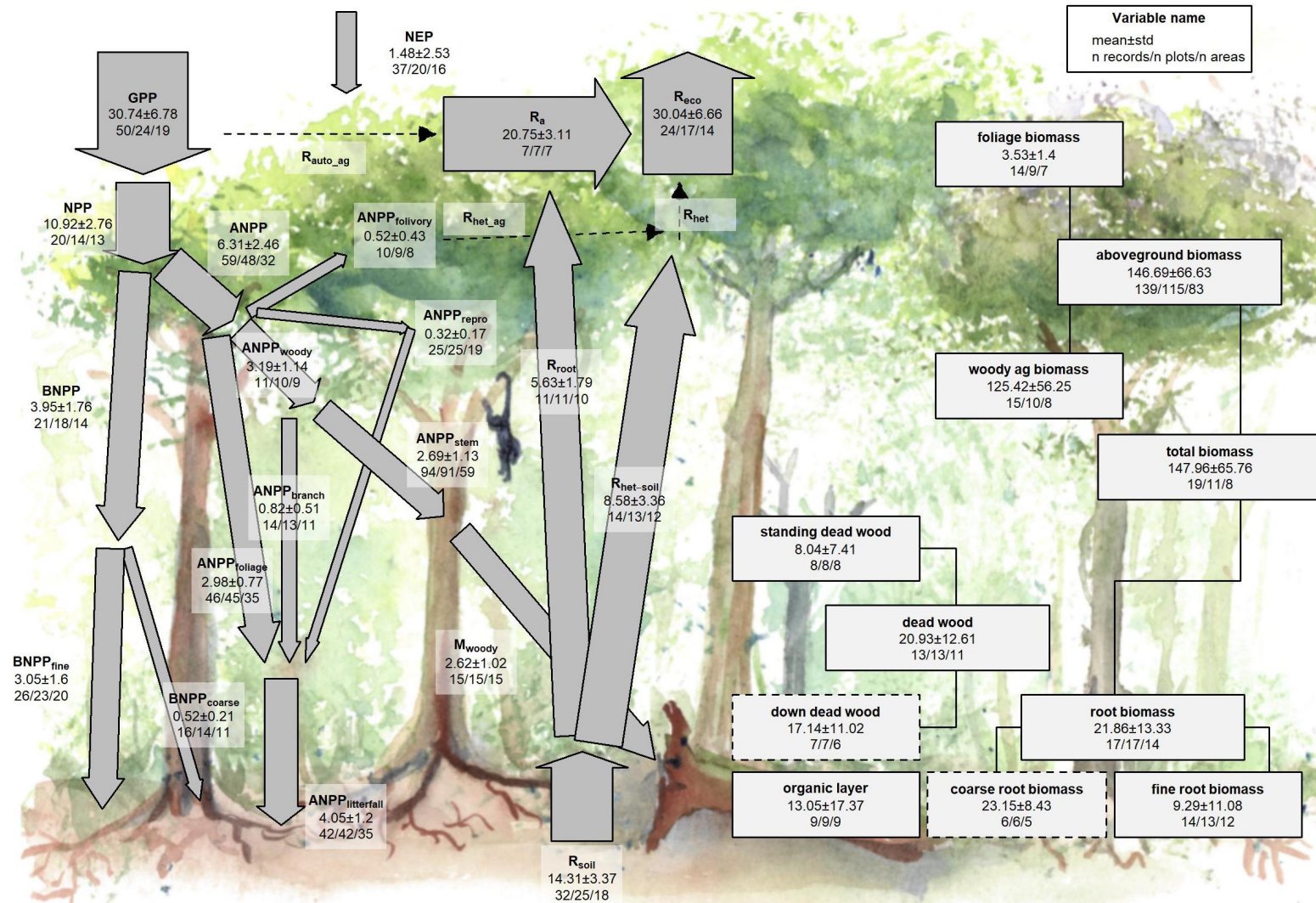
Variable name

mean±std
n records/n plots/n areas

GPP
30.74±6.78
50/24/19

NEP
1.48±2.53
37/20/16

R_{auto_ag}

R_a
20.75±3.11
7/7/7

R_{eco}
30.04±6.66
24/17/14

NPP
10.92±2.76
20/14/13

ANPP
6.31±2.46
59/48/32

$ANPP_{folivory}$
0.52±0.43
10/9/8

R_{het_ag}

R_{het}

foliage biomass
3.53±1.4
14/9/7

aboveground biomass
146.69±66.63
139/115/83

$ANPP_{repro}$
0.32±0.17
25/25/19

$ANPP_{woody}$
3.19±1.14
11/10/9

BNPP
3.95±1.76
21/18/14

R_{root}
5.63±1.79
11/11/10

woody ag biomass
125.42±56.25
15/10/8

$ANPP_{stem}$
2.69±1.13
94/91/59

total biomass
147.96±65.76
19/11/8

$ANPP_{branch}$
0.82±0.51
14/13/11

$R_{het-soil}$
8.58±3.36
14/13/12

$ANPP_{foliage}$
2.98±0.77
46/45/35

standing dead wood
8.04±7.41
8/8/8

$BNPP_{fine}$
3.05±1.6
26/23/20

M_{woody}
2.62±1.02
15/15/15

dead wood
20.93±12.61
13/13/11

$BNPP_{coarse}$
0.52±0.21
16/14/11

down dead wood
17.14±11.02
7/7/6

root biomass
21.86±13.33
17/17/14

organic layer
13.05±17.37
9/9/9

coarse root biomass
23.15±8.43
6/6/5

fine root biomass
9.29±11.08
14/13/12

$ANPP_{litterfall}$
4.05±1.2
42/42/35

R_{soil}
14.31±3.37
32/25/18

Figure 3 | C cycle diagram for mature tropical broadleaf forests. Arrows indicate fluxes (Mg C ha^{-1} yr^{-1}); boxes indicate stocks (Mg C ha^{-1}), with variables as defined in Table 1. Presented are mean ± std, where geographically distinct areas are treated as the unit of replication. Note that variables differ in geographical representation, resulting in potential imbalances (Figs. S5-S30). Probability that estimates reflect true biome means scales with the number of distinct geographical areas represented. Dashed shape outlines indicate variables with records from <7 distinct geographic areas, and dashed arrows indicate fluxes with no data. To illustrate the magnitude of different fluxes, arrow width is proportional to the square root of the corresponding flux. An asterisk after a variable name indicates lack of C cycle closure.
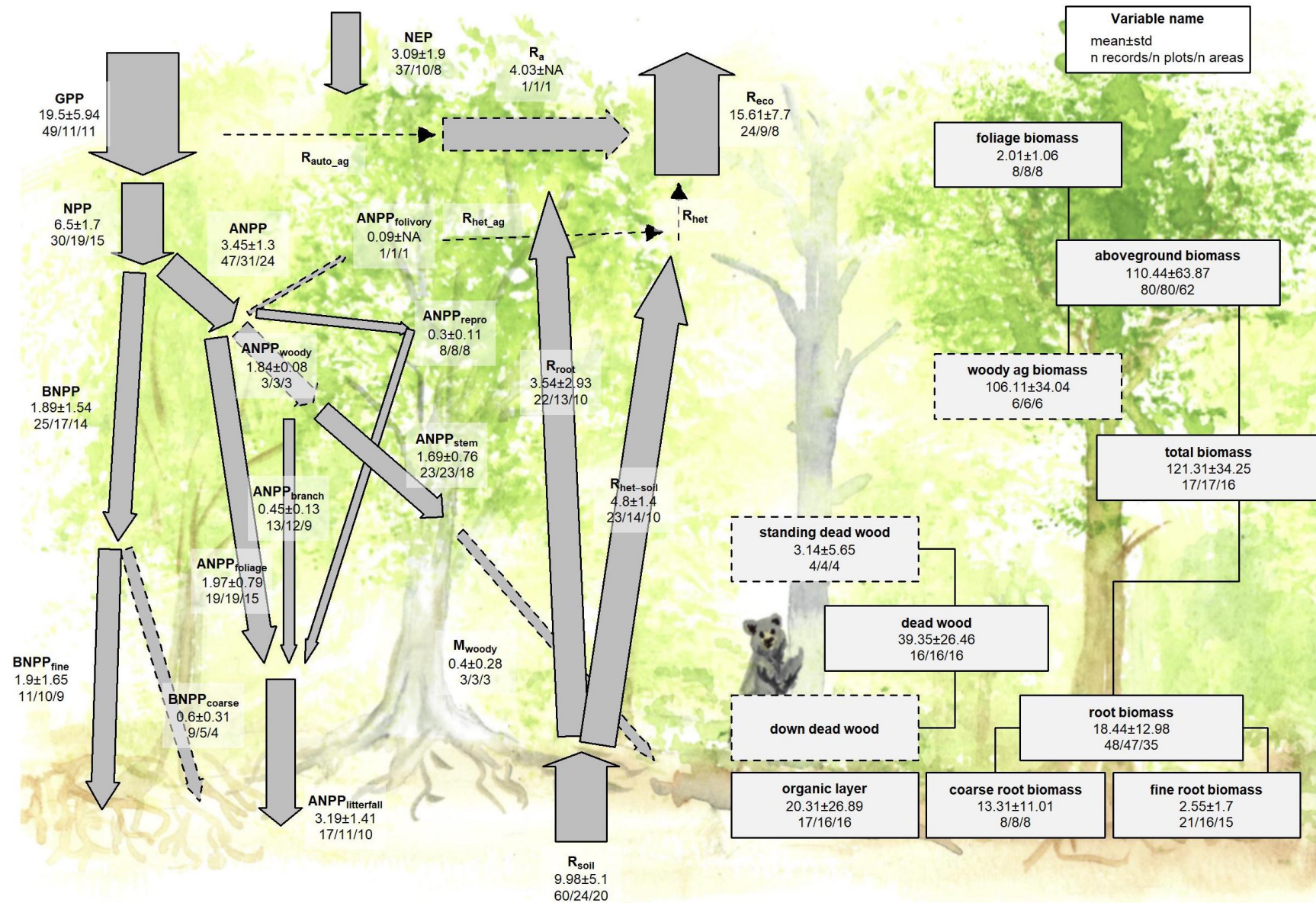
Figure 4 | C cycle diagram for mature temperate broadleaf forests. Arrows indicate fluxes (Mg C ha^{-1} yr^{-1}); boxes indicate stocks (Mg C ha^{-1}), with variables as defined in Table 1. Presented are mean ± std, where geographically distinct areas are treated as the unit of replication. Note that variables differ in geographical representation, resulting in potential imbalances (Figs. S5-S30). Probability that estimates reflect true biome means scales with the number of distinct geographical areas represented. Dashed shape outlines indicate variables with records from <7 distinct geographic areas, and dashed arrows indicate fluxes with no data. To illustrate the magnitude of different fluxes, arrow width is proportional to the square root of the corresponding flux. An asterisk after a variable name indicates lack of C cycle closure.

Variable name
mean±std
n records/n plots/n areas

NEP
0.69±1.99
35/12/11

R_a
11.66±3.93
5/5/4

GPP
13.97±4.7
44/13/10

R_{eco}
11.57±3.31
19/10/8

NPP
5.2±2.11
22/13/10

R_{auto_ag}
1.99±NA
1/1/1

ANPP
3.14±1.46
45/24/17

$ANPP_{folivory}$
0.15±NA
1/1/1

R_{het_ag}

R_{het}

foliage biomass
9.04±3.06
12/12/11

aboveground biomass
167.46±177.12
83/71/35

$ANPP_{repro}$
0.14±0.08
3/3/3

$ANPP_{woody}$
2.54±1.39
9/9/8

R_{root}
2.61±1.01
17/6/6

woody ag biomass
315.61±156.4
12/12/10

BNPP
2.03±1.37
17/10/8

$ANPP_{stem}$
1.92±1.01
16/16/12

total biomass
226.58±123.54
8/7/5

$ANPP_{branch}$
0.28±0.18
12/12/10

$R_{het-soil}$
4.36±1.23
14/8/8

$ANPP_{foliage}$
1.7±0.72
13/13/10

standing dead wood
12.83±11.58
3/3/3

dead wood
94.93±28.99
3/3/3

BNPP_fine
1.5±0.64
9/8/7

$BNPP_{coarse}$
0.89±0.57
10/10/8

M_{woody}

root biomass*
33.38±38.32
51/51/14

down dead wood

$ANPP_{litterfall}$
2.38±0.93
4/4/3

organic layer
18.97±17.85
13/9/7

coarse root biomass
77.56±58.1
16/15/12

fine root biomass
2.23±1.14
10/10/8

R_{soil}
7.11±2.51
56/26/21

Figure 5 | C cycle diagram for mature temperate conifer forests. Arrows indicate fluxes (Mg C ha^{-1} yr^{-1}); boxes indicate stocks (Mg C ha^{-1}), with variables as defined in Table 1. Presented are mean ± std, where geographically distinct areas are treated as the unit of replication. Note that variables differ in geographical representation, resulting in potential imbalances (Figs. S5-S30). Probability that estimates reflect true biome means scales with the number of distinct geographical areas represented. Dashed shape outlines indicate variables with records from <7 distinct geographic areas, and dashed arrows indicate fluxes with no data. To illustrate the magnitude of different fluxes, arrow width is proportional to the square root of the corresponding flux. An asterisk after a variable name indicates lack of C cycle closure.
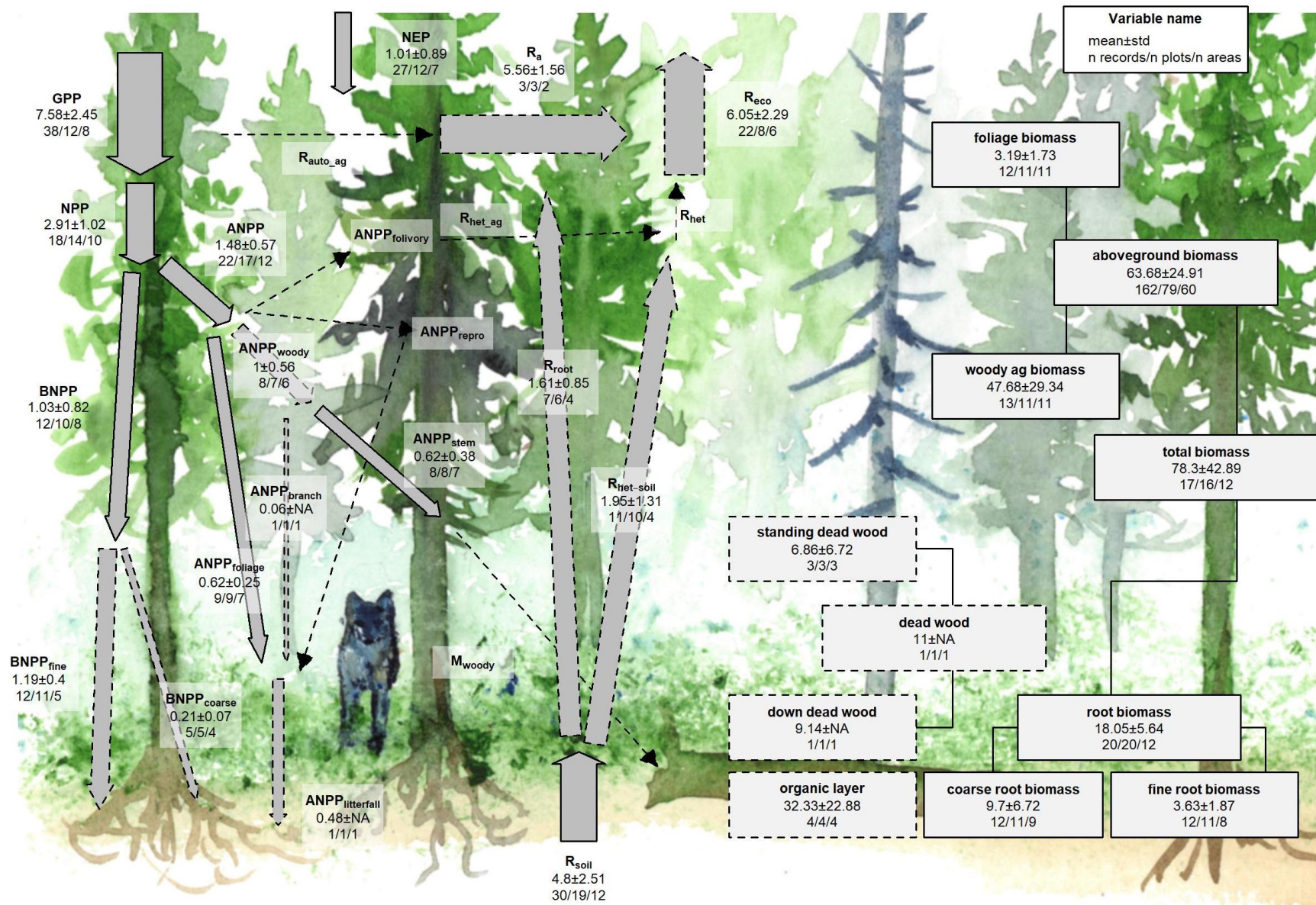
Variable name
mean±std
n records/n plots/n areas

NEP
1.01±0.89
27/12/7

Rₐ
5.56±1.56
3/3/2

Rₑ꜀ₒ
6.05±2.29
22/8/6

GPP
7.58±2.45
38/12/8

NPP
2.91±1.02
18/14/10

Rₐᵤₜₒ_ₐg

ANPP
1.48±0.57
22/17/12

ANPP_folivory

R_het_ag

R_het

BNPP
1.03±0.82
12/10/8

ANPP_woody
1±0.56
8/7/6

ANPP_repro

R_root
1.61±0.85
7/6/4

ANPP_stem
0.62±0.38
8/8/7

ANPP_branch
0.06±NA
1/1/1

R_het−soil
1.95±1.31
11/10/4

ANPP_foliage
0.62±0.25
9/9/7

foliage biomass
3.19±1.73
12/11/11

aboveground biomass
63.68±24.91
162/79/60

woody ag biomass
47.68±29.34
13/11/11

total biomass
78.3±42.89
17/16/12

standing dead wood
6.86±6.72
3/3/3

dead wood
11±NA
1/1/1

BNPP_fine
1.19±0.4
12/11/5

BNPP_coarse
0.21±0.07
5/5/4

M_woody

down dead wood
9.14±NA
1/1/1

root biomass
18.05±5.64
20/20/12

ANPP_litterfall
0.48±NA
1/1/1

organic layer
32.33±22.88
4/4/4

coarse root biomass
9.7±6.72
12/11/9

fine root biomass
3.63±1.87
12/11/8

R_soil
4.8±2.51
30/19/12

Figure 6 | C cycle diagram for mature boreaal conifer forests. Arrows indicate fluxes (Mg C ha^{-1} yr^{-1}); boxes indicate stocks (Mg C ha^{-1}), with variables as defined in Table 1. Presented are mean ± std, where geographically distinct areas are treated as the unit of replication. Note that variables differ in geographical representation, resulting in potential imbalances (Figs. S5-S30). Probability that estimates reflect true biome means scales with the number of distinct geographical areas represented. Dashed shape outlines indicate variables with records from <7 distinct geographic areas, and dashed arrows indicate fluxes with no data. To illustrate the magnitude of different fluxes, arrow width is proportional to the square root of the corresponding flux. An asterisk after a variable name indicates lack of C cycle closure.

There were sufficient data to assess differences among biomes in mature forest values for 15 flux variables, and significant differences among biomes were detected for 12 variables (Table 1). In all of these cases–including C fluxes into, within, and out of the ecosystem–C fluxes were highest in tropical forests, intermediate in temperate (broadleaf or conifer) forests, and lowest in boreal forests (Table 1, Figs. 7, S5-S19). Differences between tropical and boreal forests were always significant, with temperate forests intermediate and significantly different from one or both. Fluxes tended to be numerically greater in temperate broadleaf than temperate conifer forests, but the difference was never statistically significant. This pattern held for the following variables: GPP, NPP, $ANPP$, $ANPP_{stem}$, $ANPP_{branch}$, $ANPP_{foliage}$, $BNPP$, R_{eco}, R_{root}, R_{soil}, and $R_{het-soil}$. For two of the variables without significant differences among biomes ($ANPP_{litterfall}$ and $BNPP_{fine}$; Figs. S12 and S15, respectively), the same general trends applied but were not statistically significant. Another exception was for $BNPP_{root-coarse}$, where all records came from high-biomass forests in the US Pacific Northwest, resulting in marginally higher values for the temperate conifer biome (Table 1, Fig. S14; differences significant in mixed effects model but not in post-hoc pairwise comparison).

The most notable exception to the pattern of decreasing flux per unit area from tropical to boreal biomes was NEP, with no significant differences across biomes but with the largest average in temperate broadleaf forests, followed by tropical, boreal, and temperate conifer forests (Figs. 7, S5).
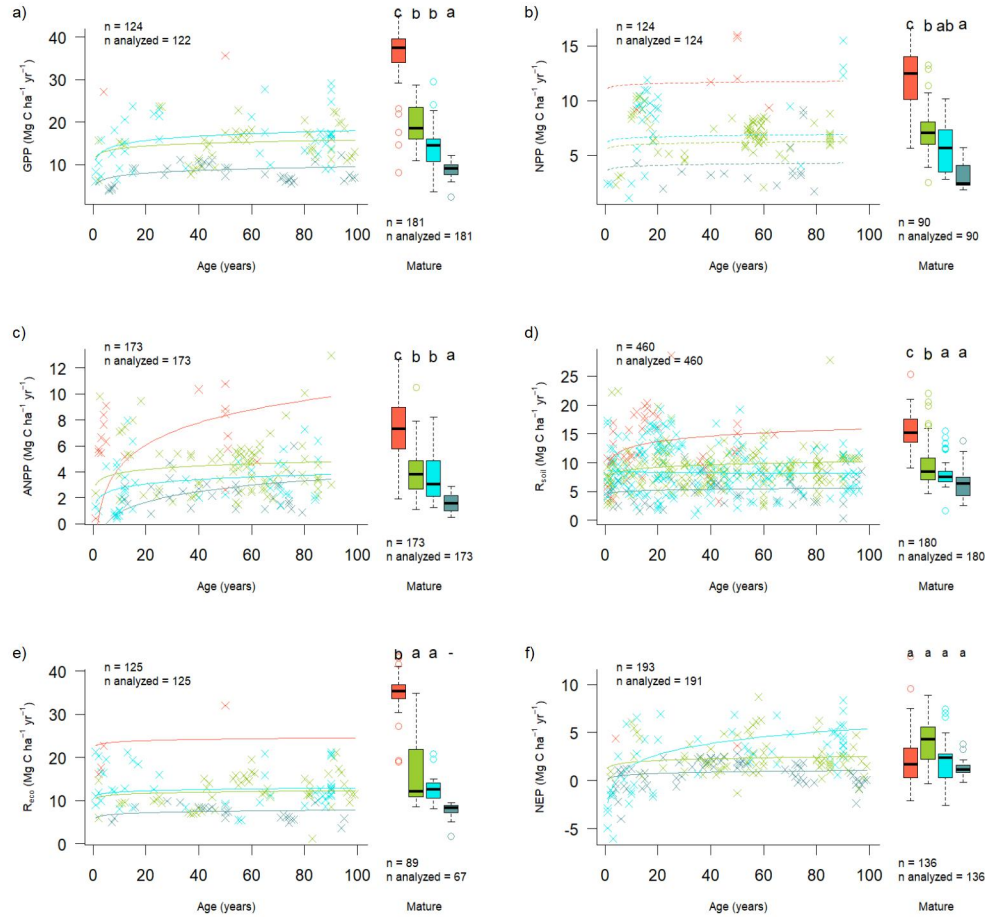
Figure 7 | Age trends and biome differences in some of the major C fluxes: (a) *GPP*, (b) *NPP*, (c) *ANPP*, (d) R_{soil}, (e) R_{eco}, and (f) *NEP*. In each panel, the left scatterplot shows age trends in forests up to 100 years old, as characterized by a linear mixed effects model with fixed effects of age and biome. The fitted line indicates the effect of age on flux (solid lines: significant at p<0.05, dashed lines: non-significant), and non-parallel lines indicate a significant age x biome interaction. The boxplot illustrates distribution across mature forests, with different letters indicating significant differences between biomes. Data from biomes that did not meet the sample size criteria (see Methods) are plotted, but lack regression lines (young forests) or test of differences across biomes (mature forests). Individual figures for each flux with sufficient data are given in the Supplement (Figs. S4-S19).

311   There were sufficient data to assess mature forest biome differences for nine stock variables, and significant

312   differences among biomes were detected for five variables (B_{tot}, B_{ag}, $B_{ag-wood}$, $B_{foliage}$, $B_{root-coarse}$; Table

313   1). C stocks had less consistent patterns across biomes (Figs. 8, S20-S30). For B_{tot} and B_{ag}, tropical

314   broadleaf forests had the highest biomass and boreal forests the lowest, with temperate broadleaf and

315   needleleaf (B_{ag} only) intermediate. For three variables that had been disproportionately sampled in the

316   high-biomass forests of the US Pacific Northwest ($B_{ag-wood}$, $B_{foliage}$, and $B_{root-coarse}$), temperate conifer

317   forests had significantly higher stocks than the other biomes, which were not significantly different from one
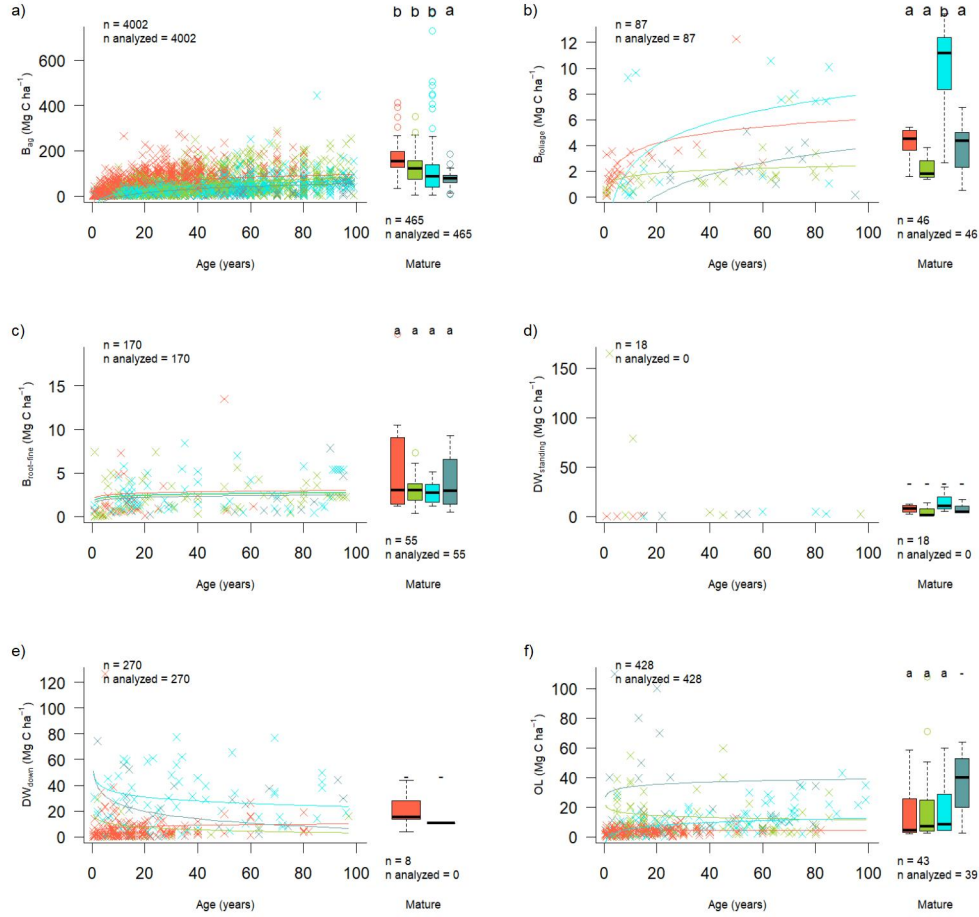
318   another.

17

Figure 8 | Age trends and biome differences in some of the major forest C stocks: (a) aboveground biomass, (b) foliage, (c) fine roots, (d) dead wood. In each panel, the left scatterplot shows age trends in forests up to 100 years old, as characterized by a linear mixed effects model with fixed effects of age and biome. The fitted line indicates the effect of age on flux (solid lines: significant at p<0.05, dashed lines: non-significant), and non-parallel lines indicate a significant age x biome interaction. The boxplot illustrates distribution across mature forests, with different letters indicating signifant differences between biomes. Data from biomes that did not meet the sample size criteria (see Methods) are plotted, but lack regression lines (young forests) or test of differences across biomes (mature forests). Individual figures for each stock with sufficient data are given in the Supplement (Figs. S20-S30).

C cycling in young forests

C fluxes commonly increased significantly with stand age (Tables 1, S2, Figs. 7, 9, S5-S30). *ForC* contained 16 C flux variables with sufficient data for analyses of age trends in young forests (see Methods). Of these, ten increased significantly with $log10[age]$: NEP, GPP, $ANPP$, $ANPP_{woody}$, $ANPP_{foliage}$, $ANPP_{litterfal}$, $BNPP$, $BNPP_{fine}$, R_{eco}, and R_{root}. The remaining six–NPP, $ANPP_{stem}$, $ANPP_{branch}$, $BNPP_{coarse}$, R_{soil}, and $R_{het-soil}$–displayed no significant relationship to stand age.
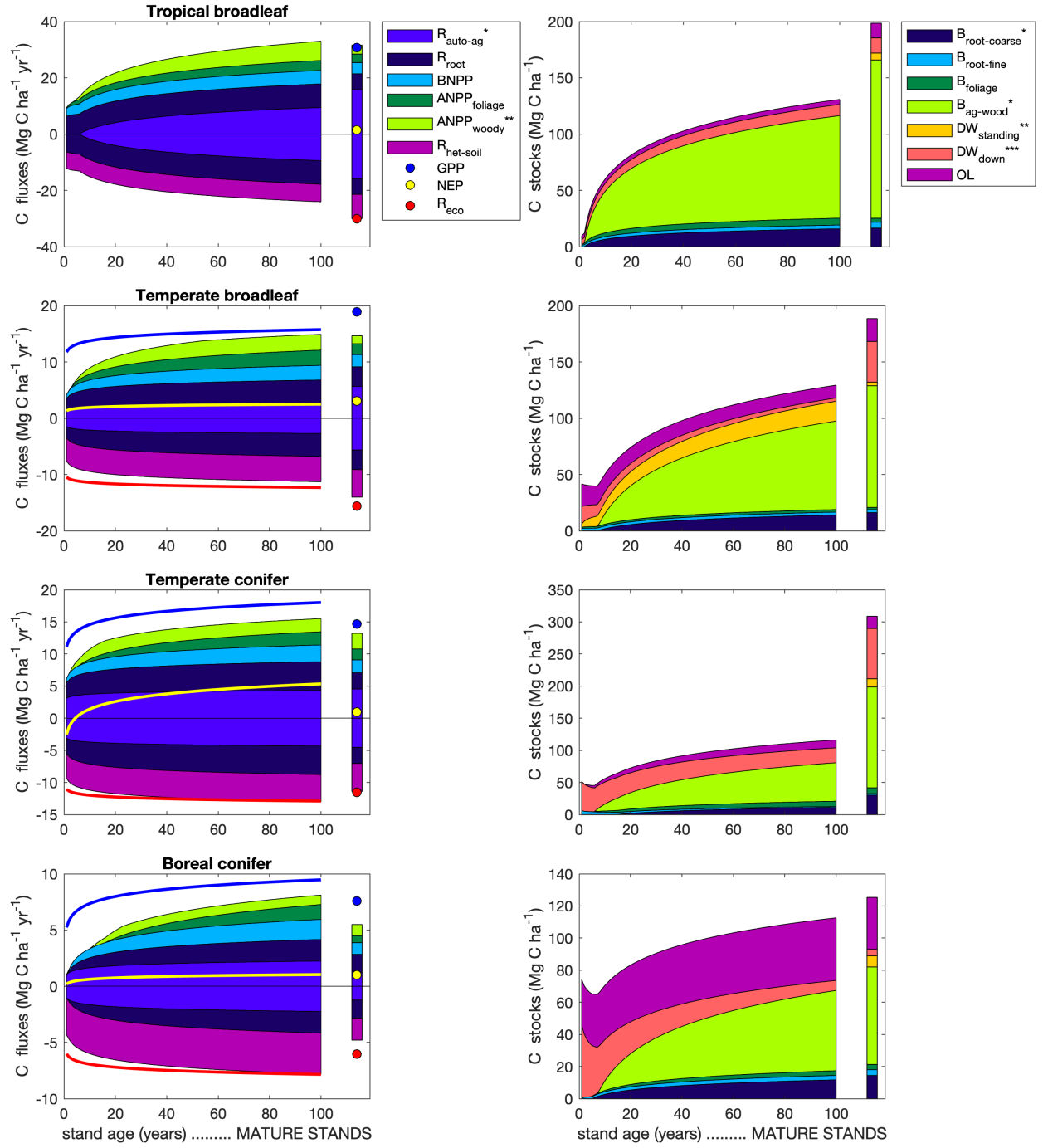
18

Figure 9 | Age trends in C cycling. Selection of variables for plotting seeks to maximize sample size and broad geographic representation while representing all elements of C cycle. Asterisks indicate variables whose age trends were calculated based on other variables (* young and mature forests; ** young forests only; *** mature forests only), as follows. For all forests: $B_{ag-wood} = max(0, B_{ag} - B_{foliage})$, $B_{root-coarse} = max(0, B_{root} - B_{root-fine})$, $DW_{standing} = max(0, DW_{tot} - DW_{down})$. For tropical forests: $ANPP_{woody} = max(0, ANPP - ANPP_{foliage})$, $R_{auto-ag} = R_{auto} - Rroot$, where $R_{auto} = NPP(1/CUE - 1)$ and CUE=0.46 (Collati et al. 2020). for non-tropical forests: $ANPP_{woody} = min(ANPP_{stem}, ANPP_{woody})$, $R_{auto-ag} = R_{eco} - Rsoil$, . Note that there remain substantial uncertainties as to the functional form of age trends and discrepencies in closure among related variables.

₃₂₅ Differences in C fluxes across biomes typically paralleled those observed for mature forests, with C cycling
₃₂₆ generally most rapid in the tropics and slowest in boreal forests. The single exception was $ANPP_{stem}$, for
₃₂₇ which temperate broadleaf and conifer forests had flux rates similar to tropical forests. Notably, and in
₃₂₈ contrast to the lack of biome differences in NEP for mature forests (Fig. 7), the tendency for temperate
₃₂₉ forests to have greater fluxes than boreal forests held for NEP in regrowth forests (tropical forests excluded
₃₃₀ because of insufficient data).

₃₃₁ "Closure" and internal consistency of the C flux budget was less successful for young than mature forests
₃₃₂ (Figs. 9). Summed regression equations for $R_{soil-het}$ and R_{root} were generally very close to R_{soil}. We
₃₃₃ calculated $R_{auto-ag}$ as the difference between R_{eco} and R_{soil} (except for tropical forests, which had
₃₃₄ insufficient R_{eco} data), effectively guaranteeing near-closure of the CO_2 efflux (respiration) portion of the
₃₃₅ budget (negative values in Figs. 9). In contrast, the CO_2 influx portion of the budget generally did not
₃₃₆ "close": the sum of R_{auto} ($R_{root} + R_{auto-ag}$, as described above) and components of NPP consistently fell
₃₃₇ short of GPP, particularly in in young stands (range across forest types and ages: 0.9-7.6 Mg C ha^{-1} yr^{-1}).
₃₃₈ Moreover, there was not consistent budget closure among the components of NPP, and substantially
₃₃₉ different age trends resulting from the sum of components versus total NPP (Figs. 9). ALthough age trends
₃₄₀ of young forests often converged towards mature forest averages, there were also some discrepancies between
₃₄₁ young forest trends and mature forest averages (Figs. 7, 9, S5-S30), most notably including a tendency for
₃₄₂ higher fluxes in regrowth boreal forests than in their mature counterparts (Fig. 9).

₃₄₃ In terms of C stocks, ten variables (all but standing deadwood, $DW_{standing}$) had sufficient data to test for
₃₄₄ age trends (Table 1, Figs. 8, S20-S30). All of these displayed a significant overall increase with with
₃₄₅ $log10[stand.age]$. There were sufficient data to model age $\times$ biome interactions were also significant for all
₃₄₆ ten of these C stock variables (Table S2), with living C stocks tending to accumulate more rapidly during the
₃₄₇ early stages of forest regrowth in tropical forests (Figs. 8, S20-S30). In the case of two non-living C stocks
₃₄₈ (DW_{down} and OL), age $\times$ biome interactions were such that Specifically, DW_{down} declined with age in
₃₄₉ temperate and boreal forests, compared to an increase with age in tropical forests (Figs. 8, S29). Similarly,
₃₅₀ OL declined slightly with age in temperate broadleaf forests, contrasting an increase in the other three
₃₅₁ biomes (Figs. 8, S30). Again, there were some discrepencies between young forest trends and mature forests,
₃₅₂ most notably including generally higher C stocks in mature forests relative to their 100-year counterparts,
₃₅₃ particularly for temperate conifer forests (*again, likely a geographic representation issue?*) and, to a lesser
₃₅₄ extent, tropical broadleaf forests.

20

Discussion

ForC v3.0 provided unprecedented coverage of most major variables, yielding a broad picture of C cycling in the world's major forest biomes. Carbon cycling rates generally increased from boreal to tropical regions and with stand age. Specifically, the major C fluxes were highest in tropical forests, intermediate in temperate (broadleaf or conifer) forests, and lowest in boreal forests – a pattern that generally held for regrowth as well as mature forests (Figs. 7- 8). In contrast to C fluxes, there was little directional variation in mature forest C stocks across biomes (Figs. 2-5, 8). The majority of flux variables, together with most live biomass pools, increased significantly with stand age (Table 1; Figs. 7- 9, S5-S30). Together, these results indicate that, moving from cold to tropical climates and from young to old stands, there is a general acceleration of C cycling, whereas C stocks and NEP of mature forests do not vary systematically across biomes. Together, these results refine and expand out understanding of C cycling in mature forests, while providing the first global-scale analysis of age trends in multiple forest C cycling stocks and fluxes (Figs. 9).

C variable coverage and budget closure

The large number of C cycle variables covered by ForC, and the general consistency among them, provide confidence that our overall reported mature forest means provide useful baselines for analysis – with the caveats that they are unlikely to be accurate representations of C cycling for any particular forest, and that these sample means almost certainly do not represent true biome means (particularly for temperate conifer forests where high-biomass stands are over-represented in *ForC*).

There are of course notable holes in the ForC variable coverage (Fig. 2) that limit the scope of our inferences here. Notably, *ForC* currently has sparse–if any–coverage of fluxes to herbivores and higher consumers, along with the woody mortality (M_{woody}) and dead wood stocks (Table 1, Figs. S27-S29). Geographically, all variables are poorly covered in Africa and Siberia, a common problem in the carbon-cycle community (Xu and Shang 2016, Schimel *et al* 2015). *ForC* does not include soil carbon, which is covered by other efforts (e.g., Köchy *et al* 2015). *ForC* is not intended to replace databases that are specialized for particular parts of the C cycle analyses, e.g., aboveground biomass (Spawn *et al* 2020), land-atmosphere fluxes (Baldocchi *et al* 2001), soil respiration (Jian *et al* 2020), or the human footprint in global forests (Magnani *et al* 2007).

In this analysis, the C cycle budgets for mature forests (Figs. 3-6) generally "close"—that is, the sums of component variables do not differ from the larger fluxes by more than one standard deviation. On the one hand, this reflects the general fact that ecosystem-scale measurements tend to close the C budget more easily and consistently than, for example, for energy balance (Stoy *et al* 2013). On the other, however, *ForC* derives data from multiple heterogeneous sources, and standard deviations within each biome are high; as a result, the standard for C closure is relatively loose (*c.f.* Houghton 2020). Nonetheless, the lack of closure, in the one instance where it occurs, is probably more reflective of differences in the representation of forest types (*i.e.*, disproportionate representation of US Pacific NW for $B_{root-coarse}$ relative to B_{root}; Fig. 5) than of methodological accuracy. The overall high degree of closure implies that *ForC* gives a consistent picture of C cycling within biomes for mature forests. This is an important and useful test, because it allows for consistency checks within the C cycle, for example leveraging separate and independently-measured fluxes to constrain errors in another (Phillips *et al* 2017, Williams *et al* 2014, Harmon *et al* 2011), or producing internally consistent global data products (Wang *et al* 2018).

In contrast, age trends for young forests generally remain less clearly defined, in large part because their data

395 records remain somewhat sparse for most variables (*i.e.*, have low representation of different geographical
396 regions for any given age). While this analysis provides a first analysis of age trends in forest C cycling for
397 multiple variables at a global scale, improved resolution of these trends will require additional data.

C cycling across biomes

399 Our analysis reveals that carbon cycling is most rapid in the tropics and slowest in boreal regions, including
400 C fluxes into (GPP), within (e.g., NPP and its components), and out of (e.g., R_{soil}, R_{eco}) the ecosystem.
401 For mature forests, this is consistent with a large body of previous work demonstrating that C fluxes
402 generally decline with latitude (or increase with temperature) on a global scale (e.g., Luyssaert *et al* 2007,
403 Gillman *et al* 2015, Li and Xiao 2019, Banbury Morgan *et al* n.d.). The consistency with which this occurs
404 across numerous fluxes is not surprising, particularly given commonality in the data analyzed or used for
405 calibration, but has never been simultaneously assessed across such a large number of variables (but see
406 Banbury Morgan *et al* n.d. for nine autotrophic fluxes).

407 The notable exception to the pattern of fluxes decreasing from tropical to boreal regions is NEP, which
408 showed no significant differences across biomes (Fig. 7f). Unlike the other C flux variables, NEP does not
409 characterize the rate at which C cycles through the ecosystem, but is the balance between C sequestration
410 (GPP) and respiratory losses (R_{eco}) and represents net CO_2 sequestration (or release) by the ecosystem (Fig.
411 1). NEP tends to be relatively small in mature forest stands (discussed further below), which accumulate
412 carbon slowly relative to younger stands, if at all (Luyssaert *et al* 2008, Amiro *et al* 2010, Besnard *et al*
413 2018). It is therefore unsurprising that there are no pronounced differences across biomes (in agreement with
414 Luyssaert *et al* 2007), suggesting that variation in NEP of mature forests is controlled less by climate and
415 more by other factors including moderate disturbances (Curtis and Gough 2018) or disequilibrium of R_{soil}
416 relative to C inputs (e.g., in peatlands where anoxic conditions inhibit decomposition; Wilson *et al* 2016).

417 In contrast to the patterns observed for NEP in mature stands, NEP of stands between 20 and 100 years of
418 age varied across biomes, being lowest in boreal forests, intermediate in temperate broadleaf forests, and
419 highest in temperate conifer forests (with insufficient data to assess tropical forests; Figs. 7, S5). This is
420 consistent with findings that live biomass accumulation rates (*e.g.*, ΔB_{ag} or ΔB_{tot}) during early secondary
421 succession decrease with latitude (Figs. 7a, S16-S22; Anderson *et al* 2006, Cook-Patton *et al* 2020). Note,
422 though, that NEP includes not only ΔB_{tot}, but also changes in DW_{tot}, OL, and soil carbon, and biome
423 differences in the accumulation rates of these variables have not been detected, in part because these
424 variables do not consistently increase with stand age (Figs. 8, S27-S30, and see discussion below;
425 Cook-Patton *et al* 2020).

426 For regrowth forests, little is known about cross-biome differences in carbon fluxes, and we are not aware of
427 any previous large-scale comparisons of C fluxes that have been limited to regrowth forests. Thus, this
428 analysis was the first to examine flux trends in regrowth forests across biomes. The observed tendency for
429 young forest fluxes to decrease from tropical to boreal regions paralleled patterns in mature forests (Figs. 7,
430 S5-S19), suggesting that regrowth forests follow latitudinal trends in carbon cycling similar to those of
431 mature forests (e.g., Banbury Morgan *et al* n.d.).

432 In contrast to C fluxes and biomass accumulation rates in regrowth forests, stocks showed less systematic
433 variation across biomes. For aboveground biomass, which is the variable in *ForC* with broadest geographical
434 representation, the modest trend of declining biomass from tropical to boreal regions mirrors observations

from spaceborne lidar that reveal a decline in aboveground biomass (for all forests, including secondary) with latitude across the N hemisphere (Hu *et al* 2016). The highest- biomass forests on Earth are, however, found in coastal temperate climates of both the southern and northern hemisphere (Figs. 1, 8a; Keith *et al* 2009, Smithwick *et al* 2002, Hu *et al* 2016). Disproportionate representation of forests in one such region–the US Pacific Northwest–inflated estimates of temperate conifer fluxes and stocks for some variables and was responsible for all of the anomalous results described here (e.g., lack of complete C budget closure, anomalous trend across biomes for $BNPP_{coarse}$). Thus, biome differences should always be interpreted relative to the geographic distribution of sampling, which only rarely covers the majority of forested area within a biome.

Whereas biomass can be remotely sensed and receives significant research attention, far less is known about geographical variation in deadwood and organic layer (OL) across biomes, which has proved a limitation for C accounting efforts (Pan *et al* 2011). Although these stocks can be important–exceeding 100 Mg C ha^{-1} in some stands (Figs. 8, S27-S29), this study is the first to synthesize deadwood data on a global scale (but see Cook-Patton *et al* 2020 for young forests). Unfortunately, data remain too sparse for statistical comparison across biomes (Figs. 8, S27-S29; but see below for age trends), pointing to a need for more widespread quantification of both standing and downed deadwood. *ForC* coverage of OL stocks is more comprehensive, revealing no significant differences across temperate and tropical biomes, but a tendency towards higher OL in boreal forests, consistent with the idea that proportionally slower decomposition in colder climates results in more buildup of organic matter (Allen *et al* 2002, Anderson-Teixeira *et al* 2011). Further research on non-living C stocks in the world's forests will be essential to completing the picture.

Age trends in C cycling

Our study reveals that most C fluxes quickly increase to a plateau as stands age (Figs. 7, 9), consistent with current understanding of age trends in forest C cycling (Fig. 1; e.g., Anderson-Teixeira *et al* 2013, Amiro *et al* 2010, Magnani *et al* 2007). While limited records in very young (*i.e.*, <5 year old) stands resulted in poor resolution of the earliest phases of this increase for many variables (sometimes detecting no age trend; Table 1), any autotrophic C flux (e.g., GPP, NPP and its components, R_{auto}) would be minimal immediately following a stand-clearing disturbance. These would be expected to increase rapidly with the most metabolically active components of biomass, foliage and fine roots, which also increase rapidly with stand age (Fig. 8). In contrast, soil heterotrophic respiration ($R_{het-soil}$) and total soil respiration (R_{soil}) are expected to be non-zero following stand-clearing disturbance, although these may decrease with a reduction of root respiration (R_{soil} only) and C exudates or increase in response to an influx of dead roots and litter (Ribeiro-Kumara *et al* 2020, Maurer *et al* 2016, Bond-Lamberty *et al* 2004). In this study, we detect no significant age trends in either variable.

Notably, net carbon sequestration (NEP) increases with age up to the 100-yr threshold examined here, with more pronounced patterns in temperate than boreal forests (Fig. 7). This finding is largely consistent with, but built from a far larger dataset than, previous studies showing an increase in NEP across relatively young stand ages (Pregitzer and Euskirchen 2004, Baldocchi *et al* 2001, Luyssaert *et al* 2008). However, NEP has been observed to decline from intermediate to old stands (Luyssaert *et al* 2008), and the NEP estimated by our model for 100-year-old temperate conifer stands (~5 Mg C ha^{-1} yr^{-1}) exceeds the mean of mature forests in the same biome (0.7 Mg C ha^{-1} yr^{-1}; Fig. 5). A decrease in NEP is consistent with the observed deceleration of biomass accumulation as stands age, although both biomass and non-living C stocks will often continue to increase well beyond the 100-yr threshold used here to delimit young and mature

stands (Luyssaert *et al* 2008, McGarvey *et al* 2014, Lichstein *et al* 2009).

In terms of stocks, our study reveals consistent increases in live biomass stocks with stand age–a pattern that is well-known and expected (e.g., Lichstein *et al* 2009, Yang *et al* 2011)–and more variable age trends in deadwood and *OL*. The latter are particularly sensitive to the type of disturbance, where disturbances that remove most organic material (e.g., logging, agriculture) result in negligible deadwood in young stands, followed by a buildup over time (tropical stands in Fig. 8; e.g., Vargas *et al* 2008). In contrast, natural disturbances (e.g., fire, drought) can produce large amounts of deadwood (mostly $DW_{standing}$) that slowly decomposes as the stand recovers, resulting in declines across young stand ages (e.g., temperate and boreal stands in Fig. 8; e.g., Carmona *et al* 2002). Again, further study and synthesis of non-living C stocks across biomes and stand ages will be valuable to giving a more comprehensive picture.

Relevance for climate change prediction and mitigation

The future of forest C cycling (Song *et al* 2019) will shape trends in atmospheric CO_2 and the course of climate change (Schimel *et al* 2015). Our findings, and more generally the data contained in *ForC* and summarized here, can help to meet two major challenges.

First, improved representation of forest C cycling in models is essential to improving predictions of the future course of climate change, for the simple reason that by definition future projections extend our existing observations and understanding to conditions that do not currently exist on Earth (McDowell *et al* 2018, Bonan and Doney 2018, Gustafson *et al* 2018). To ensure that models are giving the right answers for the right reasons (Sulman *et al* 2018), it is important to benchmark against multiple components of the C cycle that are internally consistent with each other (Collier *et al* 2018, Wang *et al* 2018). *ForC*'s tens of thousands of records are readily available in a standardized format, and our analyses here indicate that their internal consistency is reasonably high. Integration of *ForC* with models will be valuable to improving the accuracy and reliability of models (Fer *et al* 2021).

Second, *ForC* can serve as a pipeline through which information can flow efficiently from forest researchers to decision-makers working to implement forest conservation strategies at global, national, or landscape scales. This is already happening: *ForC* has contributed to updating the IPCC guidelines for carbon accounting in forests (IPCC 2019, Requena Suarez *et al* 2019), mapping C accumulation potential from natural forest regrowth globally (Cook-Patton *et al* 2020), and informing ecosystem conservation priorities (Goldstein *et al* 2020).

It is also interesting to consider the complementary utility of global-scale but spatially discontinuous databases such as ForC and remote wall-to-wall remote sensing products. The latter provide unparalleled insight into aboveground carbon stocks, but less constraint on belowground stocks or carbon fluxes in general (Bond-Lamberty *et al* 2016, Anav *et al* 2015). Combining observational data and remote observations may provide a much more comprehensive and accurate picture of global forest C cycling, particularly when used in formal data assimilation systems (Konings *et al* 2019, Liu *et al* 2018). Biomass is the largest C stock in most forests, and most of the emphasis has traditionally been on this variable. Remote-sensing driven biomass estimates (e.g., Saatchi *et al* 2011), calibrated based on high-quality ground-based data (Schepaschenko *et al* 2019, Chave *et al* 2019), are well suited for this task. Note, however, that factors such as stand age and disturbance history are difficult, if possible, to detect remotely, and can only be characterized for very recent decades (Hansen *et al* 2013, Song *et al* 2018, Curtis *et al* 2018). Ground-based

data such as *ForC* are therefore valuable in defining age-based trajectories in biomass, as in Cook-Patton *et al* (2020), and thus constraining variables such as carbon sink potential (Luyssaert *et al* 2008).

In contrast, carbon allocation within forest ecosystems and respiration fluxes cannot be remotely sensed. Efforts such as the Global Carbon Project (Friedlingstein *et al* 2019) and NASA's Carbon Monitoring System (Liu *et al* 2018) typically compute respiration as residuals of all other terms (Bond-Lamberty *et al* 2016, Harmon *et al* 2011). This means that the errors on respiration outputs are likely to be large and certainly poorly constrained, offering a unique opportunity for databases such as ForC and SRDB (Jian *et al* 2020) to provide observational benchmarks. For example, Konings *et al* (2019) produced a unique top-down estimate of global heterotrophic respiration that can both be compared with extant bottom-up estimates (Bond-Lamberty 2018) and used as an internal consistency check on other parts of the carbon cycle (Phillips *et al* 2017).

Conclusions

As climate change accelerates, understanding and managing the carbon dynamics of forests–notably including dynamics and fluxes that cannot be observed by satellites–is critical to forecasting, mitigation, and adaptation. The C data in *ForC*, as summarized here, will be valuable to these efforts. Notably, the fact that tropical forests tend to have both the highest rates of C sequestration in young stands (Fig. 8; Cook-Patton *et al* 2020), fueled by their generally high C flux rates (Table 1; Fig. 7), and the highest mean biomass (Fig. 8; Table 1; Hu *et al* 2016, Jian *et al* 2020) reinforces the concept that conservation and restoration of these forests is a priority for climate change mitigation, along with high-biomass old-growth temperate stands (Grassi *et al* 2017, Goldstein *et al* 2020). It is also important to note the trade-off in climate mitigation potential of restoration of young forests, with high rates of CO_2 sequestration (NEP; Cook-Patton *et al* 2020), versus conservation and management of mature forests, with low NEP but high C stocks that could not be recovered on a time scale relevant to climate change mitigation (Goldstein *et al* 2020). Generally speaking, the conservation of mature forests will yield greater climate benefits (Anderson-Teixeira and DeLucia 2011), but both approaches are critical to avoiding catastrophic climate change (IPCC 2018).

Citations to add

Harris *et al* (2021)

Data availability statement

Materials required to fully reproduce these analyses, including data, R scripts, and image files, are archived in Zenodo (DOI: TBD). Data, scripts, and results presented here are also available through the open-access *ForC* GitHub repository (https://github.com/forc-db/ForC), where many will be updated as the database develops.

References

Allen A, Brown J and Gillooly J 2002 Global biodiversity, biochemical kinetics, and the energetic-equivalence rule *SCIENCE* **297** 1545–8

Amiro B D, Barr A G, Barr J G, Black T A, Bracho R, Brown M, Chen J, Clark K L, Davis K J, Desai A R, Dore S, Engel V, Fuentes J D, Goldstein A H, Goulden M L, Kolb T E, Lavigne M B, Law B E, Margolis H A, Martin T, McCaughey J H, Misson L, Montes-Helu M, Noormets A, Randerson J T, Starr G and Xiao J 2010 Ecosystem carbon dioxide fluxes after disturbance in forests of North America *J. Geophys. Res.* **115** G00K02

Anav A, Friedlingstein P, Beer C, Ciais P, Harper A, Jones C, Murray-Tortarolo G, Papale D, Parazoo N C, Peylin P, Piao S, Sitch S, Viovy N, Wiltshire A and Zhao M 2015 Spatiotemporal patterns of terrestrial gross primary production: A review *Reviews of Geophysics* **53** 785–818

Andela N, Morton D C, Giglio L, Chen Y, van der Werf G R, Kasibhatla P S, DeFries R S, Collatz G J, Hantson S, Kloster S, Bachelet D, Forrest M, Lasslop G, Li F, Mangeon S, Melton J R, Yue C and Randerson J T 2017 A human-driven decline in global burned area *Science* **356** 1356–62

Anderson K J, Allen A P, Gillooly J F and Brown J H 2006 Temperature-dependence of biomass accumulation rates during secondary succession *Ecology Letters* **9** 673–82

Anderson-Teixeira K, Herrmann V, CookPatton, Ferson A and Lister K 2020 Forc-db/GROA: Release with Cook-Patton et al. 2020, Nature.

Anderson-Teixeira K J, Davies S J, Bennett A C, Gonzalez-Akre E B, Muller-Landau H C, Joseph Wright S, Abu Salim K, Almeyda Zambrano A M, Alonso A, Baltzer J L, Basset Y, Bourg N A, Broadbent E N, Brockelman W Y, Bunyavejchewin S, Burslem D F R P, Butt N, Cao M, Cardenas D, Chuyong G B, Clay K, Cordell S, Dattaraja H S, Deng X, Detto M, Du X, Duque A, Erikson D L, Ewango C E N, Fischer G A, Fletcher C, Foster R B, Giardina C P, Gilbert G S, Gunatilleke N, Gunatilleke S, Hao Z, Hargrove W W, Hart T B, Hau B C H, He F, Hoffman F M, Howe R W, Hubbell S P, Inman-Narahari F M, Jansen P A, Jiang M, Johnson D J, Kanzaki M, Kassim A R, Kenfack D, Kibet S, Kinnaird M F, Korte L, Kral K, Kumar J, Larson A J, Li Y, Li X, Liu S, Lum S K Y, Lutz J A, Ma K, Maddalena D M, Makana J-R, Malhi Y, Marthews T, Mat Serudin R, McMahon S M, McShea W J, Memiaghe H R, Mi X, Mizuno T, Morecroft M, Myers J A, Novotny V, de Oliveira A A, Ong P S, Orwig D A, Ostertag R, den Ouden J, Parker G G, Phillips R P, Sack L, Sainge M N, Sang W, Sri-ngernyuang K, Sukumar R, Sun I-F, Sungpalee W, Suresh H S, Tan S, Thomas S C, Thomas D W, Thompson J, Turner B L, Uriarte M, Valencia R, et al 2015 CTFS-ForestGEO : A worldwide network monitoring forests in an era of global change *Global Change Biology* **21** 528–49

Anderson-Teixeira K J, Delong J P, Fox A M, Brese D A and Litvak M E 2011 Differential responses of production and respiration to temperature and moisture drive the carbon balance across a climatic gradient in New Mexico *Global Change Biology* **17** 410–24

Anderson-Teixeira K J and DeLucia E H 2011 The greenhouse gas value of ecosystems *Global Change Biology* **17** 425–38

Anderson-Teixeira K J, Miller A D, Mohan J E, Hudiburg T W, Duval B D and DeLucia E H 2013 Altered dynamics of forest recovery under a changing climate *Global Change Biology* **19** 2001–21

Anderson-Teixeira K J, Wang M M H, McGarvey J C, Herrmann V, Tepley A J, Bond-Lamberty B and LeBauer D S 2018 ForC : A global database of forest carbon stocks and fluxes *Ecology* **99** 1507–7

Anderson-Teixeira K J, Wang M M H, McGarvey J C and LeBauer D S 2016 Carbon dynamics of mature and regrowth tropical forests derived from a pantropical database (TropForC-db) *Global Change Biology* **22** 1690–709

Badgley G, Anderegg L D L, Berry J A and Field C B 2019 Terrestrial gross primary production: Using NIRV to scale from site to globe *Global Change Biology* **25** 3731–40

Baldocchi D, Falge E, Gu L, Olson R, Hollinger D, Running S, Anthoni P, Bernhofer C, Davis K, Evans R, Fuentes J, Goldstein A, Katul G, Law B, Lee X, Malhi Y, Meyers T, Munger W, Oechel W, Paw K T, Pilegaard K, Schmid H P, Valentini R, Verma S, Vesala T, Wilson K and Wofsy S 2001 FLUXNET : A New Tool to Study the Temporal and Spatial Variability of EcosystemScale Carbon Dioxide, Water Vapor, and Energy Flux Densities *Bulletin of the American Meteorological Society* **82** 2415–34

Banbury Morgan B, Herrmann V, Kunert N, Bond-Lamberty B, Muller-Landau H C and Anderson-Teixeira K J Global patterns of forest autotrophic carbon fluxes *Global Change Biology*

Bates D, Mächler M, Bolker B and Walker S 2015 Fitting Linear Mixed-Effects Models Using **Lme4** *Journal of Statistical Software* **67**

Besnard S, Carvalhais N, Arain M A, Black A, de Bruin S, Buchmann N, Cescatti A, Chen J, Clevers J G P W, Desai A R, Gough C M, Havrankova K, Herold M, Hörtnagl L, Jung M, Knohl A, Kruijt B, Krupkova L, Law B E, Lindroth A, Noormets A, Roupsard O, Steinbrecher R, Varlagin A, Vincke C and Reichstein M 2018 Quantifying the effect of forest age in annual net forest carbon balance *Environmental Research Letters* **13** 124018

Bonan G B 2008 Forests and Climate Change: Forcings, Feedbacks, and the Climate Benefits of Forests *Science* **320** 1444–9

Bonan G B and Doney S C 2018 Climate, ecosystems, and planetary futures: The challenge to predict life in Earth system models *Science* **359**

Bonan G B, Lombardozzi D L, Wieder W R, Oleson K W, Lawrence D M, Hoffman F M and Collier N 2019 Model Structure and Climate Data Uncertainty in Historical Simulations of the Terrestrial Carbon Cycle (1850) *Global Biogeochemical Cycles* **33** 1310–26

Bond-Lamberty B 2018 New Techniques and Data for Understanding the Global Soil Respiration Flux *Earth's Future* **6** 1176–80

Bond-Lamberty B, Epron D, Harden J, Harmon M E, Hoffman F, Kumar J, David McGuire A and Vargas R 2016 Estimating heterotrophic respiration at large scales: Challenges, approaches, and next steps *Ecosphere* **7**

Bond-Lamberty B and Thomson A 2010 A global database of soil respiration data *Biogeosciences* **7** 1915–26

Bond-Lamberty B, Wang C and Gower S T 2004 Contribution of root respiration to soil surface CO2 flux in a boreal black spruce chronosequence *Tree Physiology* **24** 1387–95

Carmona M R, Armesto J J, Aravena J C and Pérez C A 2002 Coarse woody debris biomass in successional and primary temperate forests in Chiloé Island, Chile *Forest Ecology and Management* **164** 265–75

27

Cavaleri M A, Reed S C, Smith W K and Wood T E 2015 Urgent need for warming experiments in tropical forests *Global Change Biology* **21** 2111–21

Chapin F, Woodwell G, Randerson J, Rastetter E, Lovett G, Baldocchi D, Clark D, Harmon M, Schimel D, Valentini R, Wirth C, Aber J, Cole J, Goulden M, Harden J, Heimann M, Howarth R, Matson P, McGuire A, Melillo J, Mooney H, Neff J, Houghton R, Pace M, Ryan M, Running S, Sala O, Schlesinger W and Schulze E D 2006 Reconciling Carbon-cycle Concepts, Terminology, and Methods *Ecosystems* **9** 1041–50

Chave J, Davies S J, Phillips O L, Lewis S L, Sist P, Schepaschenko D, Armston J, Baker T R, Coomes D, Disney M, Duncanson L, Hérault B, Labrière N, Meyer V, Réjou-Méchain M, Scipal K and Saatchi S 2019 Ground Data are Essential for Biomass Remote Sensing Missions *Surveys in Geophysics*

Chave J, Réjou-Méchain M, Búrquez A, Chidumayo E, Colgan M S, Delitti W B C, Duque A, Eid T, Fearnside P M, Goodman R C, Henry M, Martínez-Yrízar A, Mugasha W A, Muller-Landau H C, Mencuccini M, Nelson B W, Ngomanda A, Nogueira E M, Ortiz-Malavassi E, Pélissier R, Ploton P, Ryan C M, Saldarriaga J G and Vieilledent G 2014 Improved allometric models to estimate the aboveground biomass of tropical trees *Global Change Biology* n/a–a

Chazdon R L, Broadbent E N, Rozendaal D M A, Bongers F, Zambrano A M A, Aide T M, Balvanera P, Becknell J M, Boukili V, Brancalion P H S, Craven D, Almeida-Cortez J S, Cabral G A L, Jong B de, Denslow J S, Dent D H, DeWalt S J, Dupuy J M, Durán S M, Espírito-Santo M M, Fandino M C, César R G, Hall J S, Hernández-Stefanoni J L, Jakovac C C, Junqueira A B, Kennard D, Letcher S G, Lohbeck M, Martínez-Ramos M, Massoca P, Meave J A, Mesquita R, Mora F, Muñoz R, Muscarella R, Nunes Y R F, Ochoa-Gaona S, Orihuela-Belmonte E, Peña-Claros M, Pérez-García E A, Piotto D, Powers J S, Rodríguez-Velazquez J, Romero-Pérez I E, Ruíz J, Saldarriaga J G, Sanchez-Azofeifa A, Schwartz N B, Steininger M K, Swenson N G, Uriarte M, Breugel M van, Wal H van der, Veloso M D M, Vester H, Vieira I C G, Bentos T V, Williamson G B and Poorter L 2016 Carbon sequestration potential of second-growth forest regeneration in the Latin American tropics *Science Advances* **2** e1501639

Chojnacky D C, Heath L S and Jenkins J C 2014 Updated generalized biomass equations for North American tree species *Forestry* **87** 129–51

Clark D A, Brown S, Kicklighter D W, Chambers J, Thomlinson J R and Ni J 2001 Measuring net primary production in forests: Concepts and field methods *Ecological Applications* **11** 356–70

Collalti A, Ibrom A, Stockmarr A, Cescatti A, Alkama R, Fernández-Martínez M, Matteucci G, Sitch S, Friedlingstein P, Ciais P, Goll D S, Nabel J E M S, Pongratz J, Arneth A, Haverd V and Prentice I C 2020 Forest production efficiency increases with growth temperature *Nature Communications* **11** 5322

Collier N, Hoffman F M, Lawrence D M, Keppel-Aleks G, Koven C D, Riley W J, Mu M and Randerson J T 2018 The International Land Model Benchmarking (ILAMB) System: Design, Theory, and Implementation *Journal of Advances in Modeling Earth Systems* **10** 2731–54

Cook-Patton S C, Leavitt S M, Gibbs D, Harris N L, Lister K, Anderson-Teixeira K J, Briggs R D, Chazdon R L, Crowther T W, Ellis P W, Griscom H P, Herrmann V, Holl K D, Houghton R A, Larrosa C, Lomax G, Lucas R, Madsen P, Malhi Y, Paquette A, Parker J D, Paul K, Routh D, Roxburgh S, Saatchi S, van den Hoogen J, Walker W S, Wheeler C E, Wood S A, Xu L and Griscom B W 2020 Mapping carbon accumulation potential from global natural forest regrowth *Nature* **585** 545–50

Corman J R, Collins S L, Cook E M, Dong X, Gherardi L A, Grimm N B, Hale R L, Lin T, Ramos J, Reichmann L G and Sala O E 2019 Foundations and Frontiers of Ecosystem Science: Legacy of a Classic Paper (Odum 1969) *Ecosystems* **22** 1160–72

Curtis P G, Slay C M, Harris N L, Tyukavina A and Hansen M C 2018 Classifying drivers of global forest loss *Science* **361** 1108–11

Curtis P S and Gough C M 2018 Forest aging, disturbance and the carbon cycle *New Phytologist*

Davies S J, Abiem I, Abu Salim K, Aguilar S, Allen D, Alonso A, Anderson-Teixeira K, Andrade A, Arellano G, Ashton P S, Baker P J, Baker M E, Baltzer J L, Basset Y, Bissiengou P, Bohlman S, Bourg N A, Brockelman W Y, Bunyavejchewin S, Burslem D F R P, Cao M, Cárdenas D, Chang L-W, Chang-Yang C-H, Chao K-J, Chao W-C, Chapman H, Chen Y-Y, Chisholm R A, Chu C, Chuyong G, Clay K, Comita L S, Condit R, Cordell S, Dattaraja H S, de Oliveira A A, den Ouden J, Detto M, Dick C, Du X, Duque Á, Ediriweera S, Ellis E C, Obiang N L E, Esufali S, Ewango C E N, Fernando E S, Filip J, Fischer G A, Foster R, Giambelluca T, Giardina C, Gilbert G S, Gonzalez-Akre E, Gunatilleke I A U N, Gunatilleke C V S, Hao Z, Hau B C H, He F, Ni H, Howe R W, Hubbell S P, Huth A, Inman-Narahari F, Itoh A, Janík D, Jansen P A, Jiang M, Johnson D J, Jones F A, Kanzaki M, Kenfack D, Kiratiprayoon S, Král K, Krizel L, Lao S, Larson A J, Li Y, Li X, Litton C M, Liu Y, Liu S, Lum S K Y, Luskin M S, Lutz J A, Luu H T, Ma K, Makana J-R, Malhi Y, Martin A, McCarthy C, McMahon S M, McShea W J, Memiaghe H, Mi X, Mitre D, Mohamad M, et al 2021 ForestGEO: Understanding forest diversity and dynamics through a global observatory network *Biological Conservation* **253** 108907

DeLucia E H, Drake J, Thomas R B and Gonzalez-Meler M A 2007 Forest carbon use efficiency: Is respiration a constant fraction of gross primary production? *Global Change Biology* **13** 1157–67

Di Vittorio A V, Shi X, Bond-Lamberty B, Calvin K and Jones A 2020 Initial Land Use/Cover Distribution Substantially Affects Global Carbon and Local Temperature Projections in the Integrated Earth System Model *Global Biogeochemical Cycles* **34**

FAO 2010 *Global Forest Resources Assessment 2010* (Rome, Italy: Food and Agriculture Organization of the United Nations)

Fer I, Gardella A K, Shiklomanov A N, Campbell E E, Cowdery E M, Kauwe M G D, Desai A, Duveneck M J, Fisher J B, Haynes K D, Hoffman F M, Johnston M R, Kooper R, LeBauer D S, Mantooth J, Parton W J, Poulter B, Quaife T, Raiho A, Schaefer K, Serbin S P, Simkins J, Wilcox K R, Viskari T and Dietze M C 2021 Beyond ecosystem modeling: A roadmap to community cyberinfrastructure for ecological data-model integration *Global Change Biology* **27** 13–26

Friedlingstein P, Cox P, Betts R, Bopp L, von Bloh W, Brovkin V, Cadule P, Doney S, Eby M, Fung I, Bala G, John J, Jones C, Joos F, Kato T, Kawamiya M, Knorr W, Lindsay K, Matthews H D, Raddatz T, Rayner P, Reick C, Roeckner E, Schnitzler K-G, Schnur R, Strassmann K, Weaver A J, Yoshikawa C and Zeng N 2006 Climate–Carbon Cycle Feedback Analysis: Results from the C4MIP Model Intercomparison *Journal of Climate* **19** 3337–53

Friedlingstein P, Jones M W, O'Sullivan M, Andrew R M, Hauck J, Peters G P, Peters W, Pongratz J, Sitch S, Quéré C L, Bakker D C E, Canadell J G, Ciais P, Jackson R B, Anthoni P, Barbero L, Bastos A, Bastrikov V, Becker M, Bopp L, Buitenhuis E, Chandra N, Chevallier F, Chini L P, Currie K I, Feely R A, Gehlen M, Gilfillan D, Gkritzalis T, Goll D S, Gruber N, Gutekunst S, Harris I, Haverd V, Houghton

R A, Hurtt G, Ilyina T, Jain A K, Joetzjer E, Kaplan J O, Kato E, Klein Goldewijk K, Korsbakken J I, Landschützer P, Lauvset S K, Lefèvre N, Lenton A, Lienert S, Lombardozzi D, Marland G, McGuire P C, Melton J R, Metzl N, Munro D R, Nabel J E M S, Nakaoka S-I, Neill C, Omar A M, Ono T, Peregon A, Pierrot D, Poulter B, Rehder G, Resplandy L, Robertson E, Rödenbeck C, Séférian R, Schwinger J, Smith N, Tans P P, Tian H, Tilbrook B, Tubiello F N, Werf G R van der, Wiltshire A J and Zaehle S 2019 Global Carbon Budget 2019 *Earth System Science Data* **11** 1783–838

Gillman L N, Wright S D, Cusens J, McBride P D, Malhi Y and Whittaker R J 2015 Latitude, productivity and species richness *Global Ecology and Biogeography* **24** 107–17

Goldstein A, Turner W R, Spawn S A, Anderson-Teixeira K J, Cook-Patton S, Fargione J, Gibbs H K, Griscom B, Hewson J H, Howard J F, Ledezma J C, Page S, Koh L P, Rockström J, Sanderman J and Hole D G 2020 Protecting irrecoverable carbon in Earth's ecosystems *Nature Climate Change* **10** 287–95

Grassi G, House J, Dentener F, Federici S, den Elzen M and Penman J 2017 The key role of forests in meeting climate targets requires science for credible mitigation *Nature Climate Change* **7** 220–6

Griscom B W, Adams J, Ellis P W, Houghton R A, Lomax G, Miteva D A, Schlesinger W H, Shoch D, Siikamäki J V, Smith P, Woodbury P, Zganjar C, Blackman A, Campari J, Conant R T, Delgado C, Elias P, Gopalakrishna T, Hamsik M R, Herrero M, Kiesecker J, Landis E, Laestadius L, Leavitt S M, Minnemeyer S, Polasky S, Potapov P, Putz F E, Sanderman J, Silvius M, Wollenberg E and Fargione J 2017 Natural climate solutions *Proceedings of the National Academy of Sciences* **114** 11645–50

Gustafson E J, Kubiske M E, Miranda B R, Hoshika Y and Paoletti E 2018 Extrapolating plot-scale CO2 and ozone enrichment experimental results to novel conditions and scales using mechanistic modeling *Ecological Processes* **7** 31

Hansen M C, Potapov P V, Moore R, Hancher M, Turubanova S A, Tyukavina A, Thau D, Stehman S V, Goetz S J, Loveland T R, Kommareddy A, Egorov A, Chini L, Justice C O and Townshend J R G 2013 High-Resolution Global Maps of 21st-Century Forest Cover Change *Science* **342** 850–3

Harmon M E, Bond-Lamberty B, Tang J and Vargas R 2011 Heterotrophic respiration in disturbed forests: A review with examples from North America *Journal of Geophysical Research* **116**

Harmon M E, Franklin J F, Swanson F J, Sollins P, Gregory S V, Lattin J D, Anderson N H, Cline S P, Aumen N G, Sedell J R, Lienkaemper G W, Cromack K and Cummins K W 1986 Ecology of Coarse Woody Debris in Temperate Ecosystems *Advances in Ecological Research* vol 15, ed A MacFadyen and E D Ford (Academic Press) pp 133–302

Harris N L, Gibbs D A, Baccini A, Birdsey R A, Bruin S de, Farina M, Fatoyinbo L, Hansen M C, Herold M, Houghton R A, Potapov P V, Suarez D R, Roman-Cuesta R M, Saatchi S S, Slay C M, Turubanova S A and Tyukavina A 2021 Global maps of twenty-first century forest carbon fluxes *Nature Climate Change* 1–7

Holdridge L R 1947 Determination of World Plant Formations From Simple Climatic Data *Science* **105** 367–8

Houghton R A 2020 Terrestrial fluxes of carbon in GCP carbon budgets *Global Change Biology* **26** 3006–14

Hu T, Su Y, Xue B, Liu J, Zhao X, Fang J and Guo Q 2016 Mapping Global Forest Aboveground Biomass with Spaceborne LiDAR, Optical Imagery, and Forest Inventory Data *Remote Sensing* **8** 565

747 Humboldt A von and Bonpland A 1807 *Essay on the Geography of Plants*

748 Hursh A, Ballantyne A, Cooper L, Maneta M, Kimball J and Watts J 2017 The sensitivity of soil respiration
749 to soil temperature, moisture, and carbon supply at the global scale *Global Change Biology* **23** 2090–103

750 IPCC 2019 *2019 Refinement to the 2006 IPCC Guidelines for National Greenhouse Gas Inventories*

751 IPCC 2018 *Global Warming of 1.5C. An IPCC Special Report on the impacts of global warming of 1.5C*
752 *above pre-industrial levels and related global greenhouse gas emission pathways, in the context of*
753 *strengthening the global response to the threat of climate change, sustainable development, and efforts to*
754 *eradicate poverty [Masson-Delmotte, V., P. Zhai, H.-O. Pörtner, D. Roberts, J. Skea, P.R. Shukla, A.*
755 *Pirani, W. Moufouma-Okia, C. Péan, R. Pidcock, S. Connors, J.B.R. Matthews, Y. Chen, X. Zhou, M.I.*
756 *Gomis, E. Lonnoy, T. Maycock, M. Tignor, and T. Waterfield (eds.)].*

757 Jian J, Vargas R, Anderson-Teixeira K, Stell E, Herrmann V, Horn M, Kholod N, Manzon J, Marchesi R,
758 Paredes D and Bond-Lamberty B 2020 *A restructured and updated global soil respiration database*
759 *(SRDB-V5)* (Data, Algorithms, and Models)

760 Johnson D J, Needham J, Xu C, Massoud E C, Davies S J, Anderson-Teixeira K J, Bunyavejchewin S,
761 Chambers J Q, Chang-Yang C-H, Chiang J-M, Chuyong G B, Condit R, Cordell S, Fletcher C, Giardina
762 C P, Giambelluca T W, Gunatilleke N, Gunatilleke S, Hsieh C-F, Hubbell S, Inman-Narahari F, Kassim
763 A R, Katabuchi M, Kenfack D, Litton C M, Lum S, Mohamad M, Nasardin M, Ong P S, Ostertag R,
764 Sack L, Swenson N G, Sun I F, Tan S, Thomas D W, Thompson J, Umaña M N, Uriarte M, Valencia R,
765 Yap S, Zimmerman J, McDowell N G and McMahon S M 2018 Climate sensitive size-dependent survival
766 in tropical trees *Nature Ecology & Evolution* 1

767 Jung M, Henkel K, Herold M and Churkina G 2006 Exploiting synergies of global land cover products for
768 carbon cycle modeling *Remote Sensing of Environment* **101** 534–53

769 Keith H, Mackey B G and Lindenmayer D B 2009 Re-evaluation of forest biomass carbon stocks and lessons
770 from the world's most carbon-dense forests *Proceedings of the National Academy of Sciences* **106**
771 11635–40

772 Konings A G, Bloom A A, Liu J, Parazoo N C, Schimel D S and Bowman K W 2019 Global satellite-driven
773 estimates of heterotrophic respiration *Biogeosciences* **16** 2269–84

774 Köchy M, Hiederer R and Freibauer A 2015 Global distribution of soil organic carbon Part 1: Masses and
775 frequency distributions of SOC stocks for the tropics, permafrost regions, wetlands, and the world *SOIL* **1**
776 351–65

777 Krause A, Pugh T A M, Bayer A D, Li W, Leung F, Bondeau A, Doelman J C, Humpenöder F, Anthoni P,
778 Bodirsky B L, Ciais P, Müller C, Murray-Tortarolo G, Olin S, Popp A, Sitch S, Stehfest E and Arneth A
779 2018 Large uncertainty in carbon uptake potential of land-based climate-change mitigation efforts *Global*
780 *Change Biology* **24** 3025–38

781 Kuzyakov Y 2006 Sources of CO2 efflux from soil and review of partitioning methods *Soil Biology and*
782 *Biochemistry* **38** 425–48

783 Li X and Xiao J 2019 Mapping Photosynthesis Solely from Solar-Induced Chlorophyll Fluorescence: A Global,
784 Fine-Resolution Dataset of Gross Primary Production Derived from OCO-2 *Remote Sensing* **11** 2563

Lichstein J W, Wirth C, Horn H S and Pacala S W 2009 Biomass Chronosequences of United States Forests: Implications for Carbon Storage and Forest Management *Old-Growth Forests* Ecological Studies ed C Wirth, G Gleixner and M Heimann (Springer Berlin Heidelberg) pp 301–41

Lieth H 1973 Primary production: Terrestrial ecosystems *Human Ecology* **1** 303–32

Liu J, Bowman K, Parazoo N C, Bloom A A, Wunch D, Jiang Z, Gurney K R and Schimel D 2018 Detecting drought impact on terrestrial biosphere carbon fluxes over contiguous US with satellite observations *Environmental Research Letters* **13** 095003

Lutz J A, Furniss T J, Johnson D J, Davies S J, Allen D, Alonso A, Anderson-Teixeira K J, Andrade A, Baltzer J, Becker K M L, Blomdahl E M, Bourg N A, Bunyavejchewin S, Burslem D F R P, Cansler C A, Cao K, Cao M, Cárdenas D, Chang L-W, Chao K-J, Chao W-C, Chiang J-M, Chu C, Chuyong G B, Clay K, Condit R, Cordell S, Dattaraja H S, Duque A, Ewango C E N, Fischer G A, Fletcher C, Freund J A, Giardina C, Germain S J, Gilbert G S, Hao Z, Hart T, Hau B C H, He F, Hector A, Howe R W, Hsieh C-F, Hu Y-H, Hubbell S P, Inman-Narahari F M, Itoh A, Janík D, Kassim A R, Kenfack D, Korte L, Král K, Larson A J, Li Y, Lin Y, Liu S, Lum S, Ma K, Makana J-R, Malhi Y, McMahon S M, McShea W J, Memiaghe H R, Mi X, Morecroft M, Musili P M, Myers J A, Novotny V, Oliveira A de, Ong P, Orwig D A, Ostertag R, Parker G G, Patankar R, Phillips R P, Reynolds G, Sack L, Song G-Z M, Su S-H, Sukumar R, Sun I-F, Suresh H S, Swanson M E, Tan S, Thomas D W, Thompson J, Uriarte M, Valencia R, Vicentini A, Vrška T, Wang X, Weiblen G D, Wolf A, Wu S-H, Xu H, Yamakura T, Yap S and Zimmerman J K 2018 Global importance of large-diameter trees *Global Ecology and Biogeography* **27** 849–64

Luyssaert S, Inglima I, Jung M, Richardson A D, Reichstein M, Papale D, Piao S L, Schulze E-D, Wingate L, Matteucci G, Aragao L, Aubinet M, Beer C, Bernhofer C, Black K G, Bonal D, Bonnefond J-M, Chambers J, Ciais P, Cook B, Davis K J, Dolman A J, Gielen B, Goulden M, Grace J, Granier A, Grelle A, Griffis T, Grünwald T, Guidolotti G, Hanson P J, Harding R, Hollinger D Y, Hutyra L R, Kolari P, Kruijt B, Kutsch W, Lagergren F, Laurila T, Law B E, Maire G L, Lindroth A, Loustau D, Malhi Y, Mateus J, Migliavacca M, Misson L, Montagnani L, Moncrieff J, Moors E, Munger J W, Nikinmaa E, Ollinger S V, Pita G, Rebmann C, Roupsard O, Saigusa N, Sanz M J, Seufert G, Sierra C, Smith M-L, Tang J, Valentini R, Vesala T and Janssens I A 2007 CO2 balance of boreal, temperate, and tropical forests derived from a global database *Global Change Biology* **13** 2509–37

Luyssaert S, Schulze E D, Borner A, Knohl A, Hessenmoller D, Law B E, Ciais P and Grace J 2008 Old-growth forests as global carbon sinks *Nature* **455** 213

Magnani F, Mencuccini M, Borghetti M, Berbigier P, Berninger F, Delzon S, Grelle A, Hari P, Jarvis P G, Kolari P, Kowalski A S, Lankreijer H, Law B E, Lindroth A, Loustau D, Manca G, Moncrieff J B, Rayment M, Tedeschi V, Valentini R and Grace J 2007 The human footprint in the carbon cycle of temperate and boreal forests *Nature* **447** 849–51

Martin P A, Newton A C and Bullock J M 2013 Carbon pools recover more quickly than plant biodiversity in tropical secondary forests *Proceedings of the Royal Society B: Biological Sciences* **280** 20132236–6

Maurer G E, Chan A M, Trahan N A, Moore D J P and Bowling D R 2016 Carbon isotopic composition of forest soil respiration in the decade following bark beetle and stem girdling disturbances in the Rocky Mountains *Plant, Cell & Environment* **39** 1513–23

McDowell N G, Allen C D, Anderson-Teixeira K, Aukema B H, Bond-Lamberty B, Chini L, Clark J S, Dietze M, Grossiord C, Hanbury-Brown A, Hurtt G C, Jackson R B, Johnson D J, Kueppers L, Lichstein J W, Ogle K, Poulter B, Pugh T A M, Seidl R, Turner M G, Uriarte M, Walker A P and Xu C 2020 Pervasive shifts in forest dynamics in a changing world *Science* **368**

McDowell N G, Michaletz S T, Bennett K E, Solander K C, Xu C, Maxwell R M and Middleton R S 2018 Predicting Chronic Climate-Driven Disturbances and Their Mitigation *Trends in Ecology & Evolution* **33** 15–27

McGarvey J C, Thompson J R, Epstein H E and Shugart H H 2014 Carbon storage in old-growth forests of the Mid-Atlantic: Toward better understanding the eastern forest carbon sink *Ecology* **96** 311–7

Novick K A, Biederman J A, Desai A R, Litvak M E, Moore D J P, Scott R L and Torn M S 2018 The AmeriFlux network: A coalition of the willing *Agricultural and Forest Meteorology* **249** 444–56

Odum E 1969 The strategy of ecosystem development *Science* **164** 262–70

Pan Y, Birdsey R A, Fang J, Houghton R, Kauppi P E, Kurz W A, Phillips O L, Shvidenko A, Lewis S L, Canadell J G, Ciais P, Jackson R B, Pacala S, McGuire A D, Piao S, Rautiainen A, Sitch S and Hayes D 2011 A Large and Persistent Carbon Sink in the World's Forests *Science* **333** 988–93

Pastorello G, Trotta C, Canfora E, Chu H, Christianson D, Cheah Y-W, Poindexter C, Chen J, Elbashandy A, Humphrey M, Isaac P, Polidori D, Ribeca A, van Ingen C, Zhang L, Amiro B, Ammann C, Arain M A, Ardö J, Arkebauer T, Arndt S K, Arriga N, Aubinet M, Aurela M, Baldocchi D, Barr A, Beamesderfer E, Marchesini L B, Bergeron O, Beringer J, Bernhofer C, Berveiller D, Billesbach D, Black T A, Blanken P D, Bohrer G, Boike J, Bolstad P V, Bonal D, Bonnefond J-M, Bowling D R, Bracho R, Brodeur J, Brümmer C, Buchmann N, Burban B, Burns S P, Buysse P, Cale P, Cavagna M, Cellier P, Chen S, Chini I, Christensen T R, Cleverly J, Collalti A, Consalvo C, Cook B D, Cook D, Coursolle C, Cremonese E, Curtis P S, D'Andrea E, da Rocha H, Dai X, Davis K J, De Cinti B, de Grandcourt A, De Ligne A, De Oliveira R C, Delpierre N, Desai A R, Di Bella C M, di Tommasi P, Dolman H, Domingo F, Dong G, Dore S, Duce P, Dufrêne E, Dunn A, Dušek J, Eamus D, Eichelmann U, ElKhidir H A M, Eugster W, Ewenz C M, Ewers B, Famulari D, Fares S, Feigenwinter I, Feitz A, Fensholt R, Filippa G, Fischer M, Frank J, Galvagno M, Gharun M, et al 2020 The FLUXNET2015 dataset and the ONEFlux processing pipeline for eddy covariance data *Scientific Data* **7** 225

Phillips C L, Bond-Lamberty B, Desai A R, Lavoie M, Risk D, Tang J, Todd-Brown K and Vargas R 2017 The value of soil respiration measurements for interpreting and modeling terrestrial carbon cycling *Plant and Soil* **413** 1–25

Poorter L, Bongers F, Aide T M, Zambrano A M A, Balvanera P, Becknell J M, Boukili V, Brancalion P H S, Broadbent E N, Chazdon R L, Craven D, Almeida-Cortez J S de, Cabral G A L, Jong B H J de, Denslow J S, Dent D H, DeWalt S J, Dupuy J M, Durán S M, Espírito-Santo M M, Fandino M C, César R G, Hall J S, Hernandez-Stefanoni J L, Jakovac C C, Junqueira A B, Kennard D, Letcher S G, Licona J-C, Lohbeck M, Marín-Spiotta E, Martínez-Ramos M, Massoca P, Meave J A, Mesquita R, Mora F, Muñoz R, Muscarella R, Nunes Y R F, Ochoa-Gaona S, Oliveira A A de, Orihuela-Belmonte E, Peña-Claros M, Pérez-García E A, Piotto D, Powers J S, Rodríguez-Velázquez J, Romero-Pérez I E, Ruíz J, Saldarriaga J G, Sanchez-Azofeifa A, Schwartz N B, Steininger M K, Swenson N G, Toledo M, Uriarte M, Breugel M van, Wal H van der, Veloso M D M, Vester H F M, Vicentini A, Vieira I C G, Bentos T V, Williamson G

B and Rozendaal D M A 2016 Biomass resilience of Neotropical secondary forests *Nature* **530** 211–4

Pregitzer K S and Euskirchen E S 2004 Carbon cycling and storage in world forests: Biome patterns related to forest age *Global Change Biology* **10** 2052–77

Pugh T A M, Lindeskog M, Smith B, Poulter B, Arneth A, Haverd V and Calle L 2019 Role of forest regrowth in global carbon sink dynamics *Proceedings of the National Academy of Sciences* **116** 4382–7

Requena Suarez D, Rozendaal D M A, Sy V D, Phillips O L, Alvarez-Dávila E, Anderson-Teixeira K, Araujo-Murakami A, Arroyo L, Baker T R, Bongers F, Brienen R J W, Carter S, Cook-Patton S C, Feldpausch T R, Griscom B W, Harris N, Hérault B, Coronado E N H, Leavitt S M, Lewis S L, Marimon B S, Mendoza A M, N'dja J K, N'Guessan A E, Poorter L, Qie L, Rutishauser E, Sist P, Sonké B, Sullivan M J P, Vilanova E, Wang M M H, Martius C and Herold M 2019 Estimating aboveground net biomass change for tropical and subtropical forests: Refinement of IPCC default rates using forest plot data *Global Change Biology* **25** 3609–24

Ribeiro-Kumara C, Köster E, Aaltonen H and Köster K 2020 How do forest fires affect soil greenhouse gas emissions in upland boreal forests? A review *Environmental Research* **184** 109328

Saatchi S S, Harris N L, Brown S, Lefsky M, Mitchard E T A, Salas W, Zutta B R, Buermann W, Lewis S L, Hagen S, Petrova S, White L, Silman M and Morel A 2011 Benchmark map of forest carbon stocks in tropical regions across three continents *Proceedings of the National Academy of Sciences* **108** 9899–904

Schepaschenko D, Chave J, Phillips O L, Lewis S L, Davies S J, Réjou-Méchain M, Sist P, Scipal K, Perger C, Herault B, Labrière N, Hofhansl F, Affum-Baffoe K, Aleinikov A, Alonso A, Amani C, Araujo-Murakami A, Armston J, Arroyo L, Ascarrunz N, Azevedo C, Baker T, Bałazy R, Bedeau C, Berry N, Bilous A M, Bilous S Y, Bissiengou P, Blanc L, Bobkova K S, Braslavskaya T, Brienen R, Burslem D F R P, Condit R, Cuni-Sanchez A, Danilina D, Torres D del C, Derroire G, Descroix L, Sotta E D, d'Oliveira M V N, Dresel C, Erwin T, Evdokimenko M D, Falck J, Feldpausch T R, Foli E G, Foster R, Fritz S, Garcia-Abril A D, Gornov A, Gornova M, Gothard-Bassébé E, Gourlet-Fleury S, Guedes M, Hamer K C, Susanty F H, Higuchi N, Coronado E N H, Hubau W, Hubbell S, Ilstedt U, Ivanov V V, Kanashiro M, Karlsson A, Karminov V N, Killeen T, Koffi J-C K, Konovalova M, Kraxner F, Krejza J, Krisnawati H, Krivobokov L V, Kuznetsov M A, Lakyda I, Lakyda P I, Licona J C, Lucas R M, Lukina N, Lussetti D, Malhi Y, Manzanera J A, Marimon B, Junior B H M, Martinez R V, Martynenko O V, Matsala M, Matyashuk R K, Mazzei L, Memiaghe H, Mendoza C, Mendoza A M, Moroziuk O V, Mukhortova L, Musa S, Nazimova D I, Okuda T, Oliveira L C, et al 2019 The Forest Observation System, building a global reference dataset for remote sensing of forest biomass *Scientific Data* **6** 1–11

Schimel D, Hargrove W, Hoffman F and MacMahon J 2007 NEON: A hierarchically designed national ecological network *Frontiers in Ecology and the Environment* **5** 59–9

Schimel D, Stephens B B and Fisher J B 2015 Effect of increasing CO_2 on the terrestrial carbon cycle *Proceedings of the National Academy of Sciences* **112** 436–41

Smithwick E A H, Harmon M E, Remillard S M, Acker S A and Franklin J F 2002 Potential upper bounds of carbon stores in forests of the Pacific Northwest *Ecological Applications* **12** 1303–17

Song J, Wan S, Piao S, Knapp A K, Classen A T, Vicca S, Ciais P, Hovenden M J, Leuzinger S, Beier C, Kardol P, Xia J, Liu Q, Ru J, Zhou Z, Luo Y, Guo D, Adam Langley J, Zscheischler J, Dukes J S, Tang

J, Chen J, Hofmockel K S, Kueppers L M, Rustad L, Liu L, Smith M D, Templer P H, Quinn Thomas R, Norby R J, Phillips R P, Niu S, Fatichi S, Wang Y, Shao P, Han H, Wang D, Lei L, Wang J, Li X, Zhang Q, Li X, Su F, Liu B, Yang F, Ma G, Li G, Liu Y, Liu Y, Yang Z, Zhang K, Miao Y, Hu M, Yan C, Zhang A, Zhong M, Hui Y, Li Y and Zheng M 2019 A meta-analysis of 1,119 manipulative experiments on terrestrial carbon-cycling responses to global change *Nature Ecology & Evolution* **3** 1309–20

Song X-P, Hansen M C, Stehman S V, Potapov P V, Tyukavina A, Vermote E F and Townshend J R 2018 Global land change from 1982 to 2016 *Nature* **560** 639–43

Spawn S A, Sullivan C C, Lark T J and Gibbs H K 2020 Harmonized global maps of above and belowground biomass carbon density in the year 2010 *Scientific Data* **7** 112

Stoy P C, Mauder M, Foken T, Marcolla B, Boegh E, Ibrom A, Arain M A, Arneth A, Aurela M, Bernhofer C, Cescatti A, Dellwik E, Duce P, Gianelle D, van Gorsel E, Kiely G, Knohl A, Margolis H, McCaughey H, Merbold L, Montagnani L, Papale D, Reichstein M, Saunders M, Serrano-Ortiz P, Sottocornola M, Spano D, Vaccari F and Varlagin A 2013 A data-driven analysis of energy balance closure across FLUXNET research sites: The role of landscape scale heterogeneity *Agricultural and Forest Meteorology* **171-172** 137–52

Sulman B N, Moore J A M, Abramoff R, Averill C, Kivlin S, Georgiou K, Sridhar B, Hartman M D, Wang G, Wieder W R, Bradford M A, Luo Y, Mayes M A, Morrison E, Riley W J, Salazar A, Schimel J P, Tang J and Classen A T 2018 Multiple models and experiments underscore large uncertainty in soil carbon dynamics *Biogeochemistry* **141** 109–23

Taylor P G, Cleveland C C, Wieder W R, Sullivan B W, Doughty C E, Dobrowski S Z and Townsend A R 2017 Temperature and rainfall interact to control carbon cycling in tropical forests ed L Liu *Ecology Letters* **20** 779–88

Team R C 2020 R : A language and environment for statistical computing. R Foundation for Statistical Computing, Vienna, Austria. URL http://www.R-project.org/.

Tubiello F N, Pekkarinen A, Marklund L, Wanner N, Conchedda G, Federici S, Rossi S and Grassi G 2020 Carbon Emissions and Removals by Forests: New Estimates 1990–2020 *Earth System Science Data Discussions* 1–21

van der Werf G R, Randerson J T, Giglio L, van Leeuwen T T, Chen Y, Rogers B M, Mu M, van Marle M J E, Morton D C, Collatz G J, Yokelson R J and Kasibhatla P S 2017 Global fire emissions estimates during 1997 *Earth System Science Data* **9** 697–720

Vargas R, Allen M F and Allen E B 2008 Biomass and carbon accumulation in a fire chronosequence of a seasonally dry tropical forest *Global Change Biology* **14** 109–24

Wang Y, Ciais P, Goll D, Huang Y, Luo Y, Wang Y-P, Bloom A A, Broquet G, Hartmann J, Peng S, Penuelas J, Piao S, Sardans J, Stocker B D, Wang R, Zaehle S and Zechmeister-Boltenstern S 2018 GOLUM-CNP v1.0: A data-driven modeling of carbon, nitrogen and phosphorus cycles in major terrestrial biomes *Geoscientific Model Development* **11** 3903–28

Warner D L, Bond-Lamberty B, Jian J, Stell E and Vargas R 2019 Spatial Predictions and Associated Uncertainty of Annual Soil Respiration at the Global Scale *Global Biogeochemical Cycles* **33** 1733–45

942 Williams C A, Collatz G J, Masek J, Huang C and Goward S N 2014 Impacts of disturbance history on
943   forest carbon stocks and fluxes: Merging satellite disturbance mapping with forest inventory data in a
944   carbon cycle model framework *Remote Sensing of Environment* **151** 57–71

945 Wilson R M, Hopple A M, Tfaily M M, Sebestyen S D, Schadt C W, Pfeifer-Meister L, Medvedeff C,
946   McFarlane K J, Kostka J E, Kolton M, Kolka R K, Kluber L A, Keller J K, Guilderson T P, Griffiths N
947   A, Chanton J P, Bridgham S D and Hanson P J 2016 Stability of peatland carbon to rising temperatures
948   *Nature Communications* **7** 13723

949 Xu M and Shang H 2016 Contribution of soil respiration to the global carbon equation *Journal of Plant*
950   *Physiology* **203** 16–28

951 Yang Y, Luo Y and Finzi A C 2011 Carbon and nitrogen dynamics during forest stand development: A
952   global synthesis *New Phytologist* **190** 977